

Fig. 2. HSP90 inhibitors reverse Core-induced growth inhibition in yeast cells. (A) Yeast cells carrying the pRS425-GAL1-core plasmid were cultured with (+) and without (-) 3% galactose plus geldanamycin, herbimycin A, herbimycin B, herbimycin C (0.1–400 μg/ml), or radicicol (0.1–100 μg/ml) as indicated for 72 h at 30 °C. As a control, cells were cultured without the antibiotics (0). (B) Growth recovery% in the presence of 10 μg/ml radicicol for 36 h at 30 °C. The percentage of the growth recovery was 35%. The data shown are the mean ± S.D. of three independent experiments. (C) Effect of radicicol on the level of Core protein in yeast cells. Yeast cells carrying the pRS425-GAL1-core plasmid were cultured with (+) or without (-) 1 μg/ml radicicol in the presence of 3% galactose for 72 h at 30 °C. Photographs of immunoblots using Core-specific and actin-specific antibodies. (D) Effects of radicicol (1, 5 and 10 μg/ml) on the level of Core RNA as determined by northern blotting. Total RNA was prepared from yeast cells 2 h after induction of Core protein expression. Effects of radicicol on galactose-induced Gal4-dependent transcription of Core (*Core*) and *GAL1* (*GAL1*) were examined by hybridization with probes to detect Core, *GAL1* and *ACT1* RNAs. Ribosomal RNA was visualized by staining with ethidium bromide.

2.4. Preparation of cell lysates and western blotting

We examined the Core by western blotting as described previously [12] and in the Supplemental Information. We used primary antibodies specific for actin (sc-1616; Santa Cruz Biotechnology, Santa Cruz, CA, USA), Hsp90 (K41110, from Dr. Nemoto) [13,14], and Core (515S) [15].

2.5. Analysis of the distribution of the Core in yeast cells using GFP-core proteins and immunofluorescence

Core in yeast were examined by indirect immunofluorescence as described previously [16] and in the Supplemental Information. Yeast cells expressing core proteins carrying pKT10-GAL1-GFP-core¹⁹¹ and pKT10-GAL1-GFP-core¹⁷⁷ were analyzed using confocal microscopy (Olympus FV1000).

2.6. Statistical analysis

Multiple independent replicates ($n=3$, except as indicated) were performed for each experiment, and data are presented as the mean of three independent experiments with the standard deviation (SD).

3. Results

3.1. Inhibition of yeast cell growth by expressing Core

Yeast cell growth was significantly inhibited when the full-length core of HCV 1b (aa 1–191; Core) was expressed under the control of the inducible *GAL1* promoter (Fig. 1B). Core of the HCV 2a (JFH1) genotype had a similar effect, suggesting that the conserved

HCV core structure from different strains may be responsible for the core protein's effect on yeast cells. The C-terminal region of Core includes a domain (D2: aa 118–171) (Fig. 1A) that is responsible for association with the ER and lipid droplets [5] and a Core-E1 signal peptide (aa 178–191) [17]. We examined the distribution of Core on ER in yeast. Immunofluorescent microscopy indicated that Core localized on the periphery of the nucleus (Fig. 1C). The D2 domain fused to GFP (GFP-Core) co-localized with Hmg2 as an ER marker [18] (Hmg2-mCherry; Fig. 1D) in live yeast cells (Fig. 1E) and showed a reticular fluorescence pattern and cell periphery.

3.2. Inhibitors of HSP90 reduce Core stability in yeast cells

We postulated that if the proliferation of yeast cells expressing Core could be restored by treatment with certain compounds, it might provide clues regarding the cytotoxic effect of Core on yeast cells. We screened various antibiotics isolated from fungi and actinomycetes and found that inhibitors of HSP90 were able to suppress Core toxicity. The compounds determined to exhibit this suppressive activity included geldanamycin (300 and 400 μg/ml), radicicol (0.5, 1 and 10 μg/ml), herbimycin A (100–400 μg/ml) and herbimycin C (100 and 200 μg/ml), but not herbimycin B (Fig. 2A; Core (-)). Radicicol was more effective at lower concentrations than the other inhibitors, so we focused on its effects (Fig. 2A). Treatment with 10 μg/ml radicicol for 36 h restored yeast cell growth (Fig. 2B). HSP90 inhibitors inhibit HSP90/HSC90 ATPase activity by competing with ATP for binding and thereby eliminate HSP90/HSC90 chaperone activity [19]. This chaperone activity may affect expression of the Core. The level of the Core in

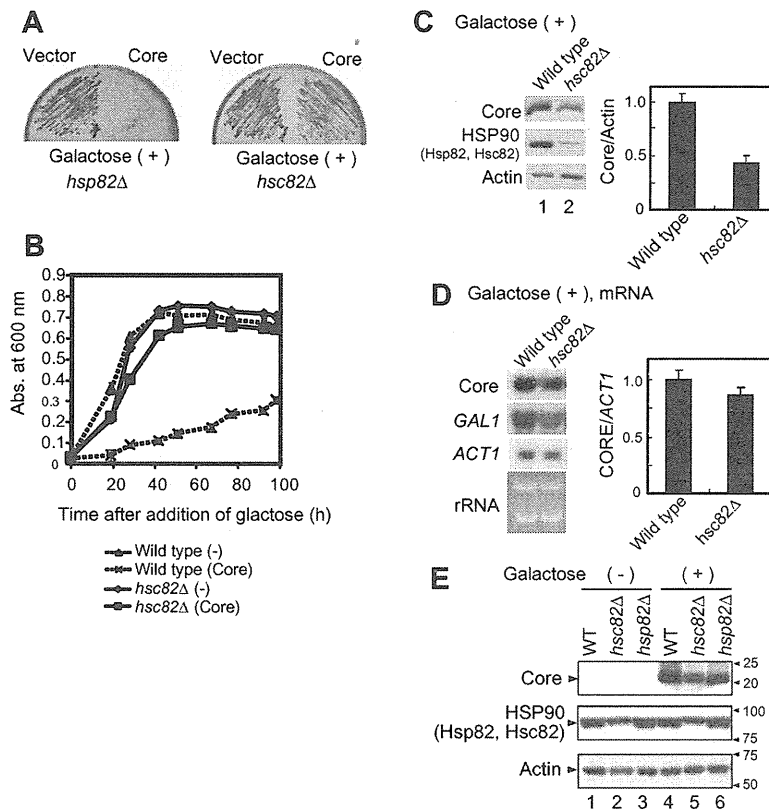


Fig. 3. Effects of HSP90 on the stability of Core in yeast cells. (A) Disruption of *HSC82*, but not *HSP82* reversed the growth inhibition induced by Core. (B) Growth curve of core-expressing *hsc82Δ* yeast cells. We examined the time-dependent absorbance at 600 nm of BY4742 (Wild type) and *hsp82Δ* yeast cells carrying pRS425-GAL1-core for 96 h after addition of 3% galactose (Core) or without addition of galactose (-). (C and D) Effects of *HSC82* disruption on Core (C) and Core RNA (D) levels in yeast cells that were monitored as in Fig. 2. (E) Effects of the levels of all Hsp82/Hsc82 proteins on Core levels. Mutant yeast cells with a disrupted *HSC82* or *HSP82* gene harboring pRS425-GAL1-core were cultured with (+) or without (-) 3% galactose for 72 h (A) or 2 h (C–E) at 30 °C. We used a monoclonal antibody that reacts with the Ic epitope common to Hsc82 and Hsp82 [14].

radicicol-treated yeast cells (1 μg/ml) was 36% of control levels (Fig. 2C) whereas the level of Core mRNA did not change (Fig. 2D).

3.3. The HSC90 ortholog Hsc82 is responsible for the Core toxicity

An HSP90 family member (HSP90/HSC90) is a highly conserved molecular chaperone that can induce the maturation of various proteins, including kinases, transcription factors, and proteins, that function in signal transduction (for review, see [20]). To identify the *HSP90* gene that affects Core levels, we disrupted HSP90 family member (*HSP82* and *HSC82*) genes in yeast [21] and examined growth in the presence of Core. Disruption of *HSC82* (*hsc82Δ*) but not of *HSP82* (*hsp82Δ*) alleviated some of the negative effects of the Core on cell growth (Fig. 3A). The effect of *HSC82* disruption was also clear in liquid culture: the growth rate of Core-expressing *hsc82Δ* cells was similar to that of wild-type cells and of *hsc82Δ* cells not expressing Core (Fig. 3B). In addition, the Core levels in *hsc82Δ* cells decreased to 44% of the level in control cells (Fig. 3C), but the level of Core mRNA was only slightly lower (Fig. 3D). The total levels of HSP90 family proteins (Hsc82 and Hsp82) decreased to 18% of the levels in control cells (Fig. 3C, compare lanes 1 and 2 of the left panel) after disruption of the *HSC82* gene, indicating that the principal HSP90 family protein (at steady state) in yeast is Hsc82, as previously reported [21]. Furthermore, neither heat-inducible Hsp82 protein levels (compare lanes 2 and 5 in Fig. 3E) nor total HSP90 family protein levels (compare lanes

1 and 4) were increased in response to induced Core expression. There was a correlation between the effects of radicicol and disruption of *HSC82*, suggesting that total HSP90 family protein levels (activity) may be involved in modulating Core levels and thereby contribute to the Core protein's growth-inhibitory effects.

3.4. An HSP90 family protein is required for stability of the nascent Core

To examine whether the Core degradation rate is affected by disruption of *HSC82*, we treated cells expressing the Core with cycloheximide (CHX) and examined the time-dependent decay of the core protein. As shown in Fig. 4A, the Core degradation rate was significantly greater when *HSC82* was disrupted. This greater degradation rate was also observed when cells were pretreated with radicicol prior to CHX treatment (Fig. 4B). In contrast, there was no significant difference in the Core degradation rate when cells were treated with radicicol and CHX simultaneously (Fig. 4C). These results suggest that the degradation rate of nascent Core may be enhanced when the levels of HSP90 family members are reduced or the activity of HSP90 family members is inhibited. However, the stability of Core produced in the presence of a wild-type level of activity of HSP90 family members was not affected by HSP90 inhibitors. Our results suggest that HSP90/HSC90 may be essential for protecting nascent Core from degradation during protein synthesis.

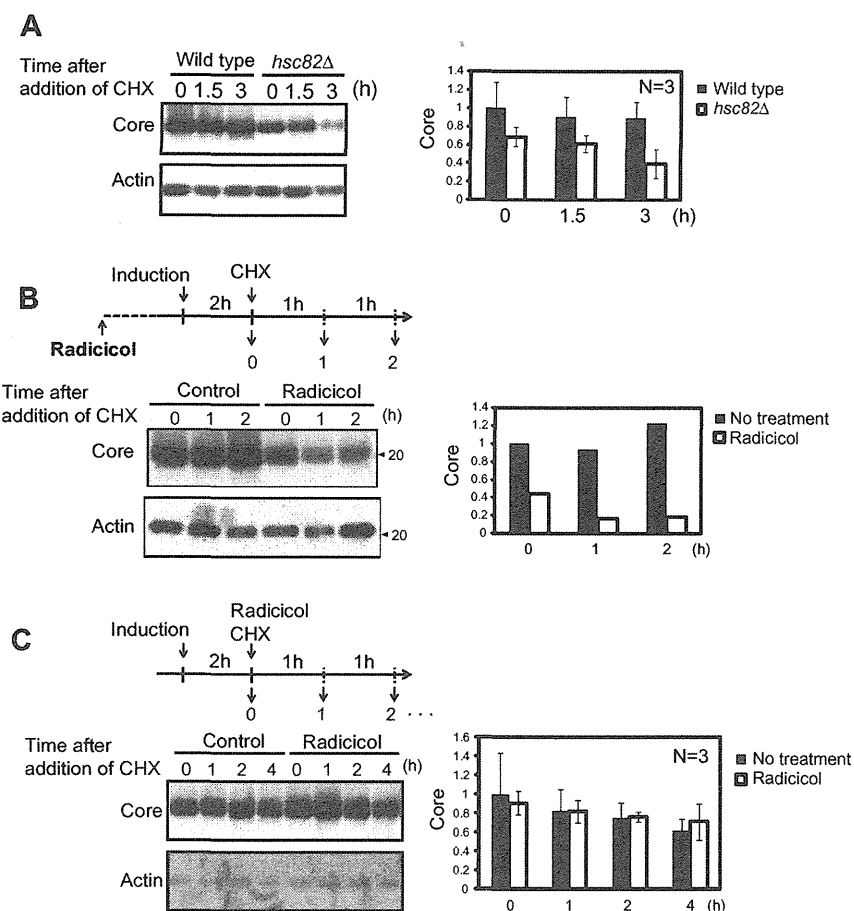


Fig. 4. Instability of nascent Core in yeast cells with reduced HSP90 activity. (A) Effect of *HSC82* disruption on Core stability. We cultured wild-type and *hsc82Δ* yeast cells carrying pRS425-GAL1-core with 3% galactose for 2 h (0 h) and then further incubated (chased) the cells with 300 mM cycloheximide (CHX) for 1.5 h and 3 h. Core and actin were separated by SDS-PAGE and quantified by western blotting. (B) Pretreatment with radicicol had an effect similar to that of *hsc82* disruption. Wild-type yeast cells carrying pRS425-GAL1-core were treated with radicicol (1 μ g/ml) for 12 h and then cultured with 3% galactose for 2 h. Core was chased as in (A). (C) Simultaneous treatment with radicicol and CHX did not alter Core stability. We treated wild-type yeast cells expressing Core with radicicol (1 μ g/ml) and CHX (0.1 mg/ml) to examine their effects on Core stability. Means from experiments performed in triplicate are indicated (A and C), and representative data (B) are presented in bar graphs.

3.5. The Core D2 domain contributes to HSC90-dependent stability and association with the ER

The Core-E1 signal peptide in the full-length Core is efficiently cleaved by a signal peptide peptidase to form Core¹⁷⁷ in human hepatoma cells [17]. This Core-processing activity is significantly lower in yeast (data not shown). Thus, we expressed Core¹⁷⁷ and examined its stability. We found that yeast cell growth was also impaired by Core¹⁷⁷ (Fig. 5A). As shown in Fig. 5B, we discovered that the rate of Core¹⁷⁷ degradation was accelerated in *HSC82*-disrupted cells. The D2 domain includes two amphipathic α -helices with the potential ability to interact with lipid droplets as well as the ER [9]. We examined whether the Core D2 domain is responsible for Hsc82-dependent stability of the Core. The degradation rate of GFP fused to a region containing the D2 domain and the signal peptide (aa 125–191; GFP-Core) and GFP fused to the D2 domain with the processed signal peptide (aa 125–177; GFP-Core¹⁷⁷) increased twofold when *HSC82* was disrupted (Figs. 5B–D). Interestingly, the Hsc82-dependent stability of Core¹⁷⁷ was comparable to that of GFP-Core¹⁷⁷. However, GFP-Core was the most stable form in the absence of Hsc82 (Fig. 5E).

We examined the distribution of GFP-Core¹⁷⁷ in yeast. GFP-Core¹⁷⁷ was detected in small particles in the perinuclear region, although it also co-localized with Hmg2-mCherry (Fig. 6A). These

results suggest that the ER-D2 domain interaction might affect the distribution of ER-localized Hmg2 proteins or the structure of the ER membrane itself. In addition to the observed puncta, GFP-Core¹⁷⁷ was distributed throughout the cytoplasm (compare Fig. 6A and Fig. 1E). Next, to demonstrate the effect of *HSC82* disruption on the distribution and degradation of GFP-Core proteins, we obtained time-lapse fluorescent images of GFP-Core after suppressing its expression; the *GAL4* promoter was suppressed by addition of glucose (Figs. 6B and C). Disruption of *HSC82* did not affect the localization of either GFP-Core or GFP-Core¹⁷⁷, but the degradation rates were again enhanced. Our results suggest a contribution of the D2 domain to the ER localization and the HSP90/HSC90-dependent stability of the Core. In fact, the intracellular levels (Fig. 7A) and the stability of a truncated Core (aa 1–151; Core¹⁵¹; Fig. 7B), in which a half of D2 was removed, were significantly decreased (the half-life was less than 0.5 h). The yeast cell growth was not affected by expression of Core¹⁵¹ (Fig. 7B). Thus, the stabilities (expression levels) of core might determine the growth inhibition.

4. Discussion

Here, we demonstrate that the Core impairs growth in yeast and that HSC90 is required for Core stabilization in yeast cells. Our

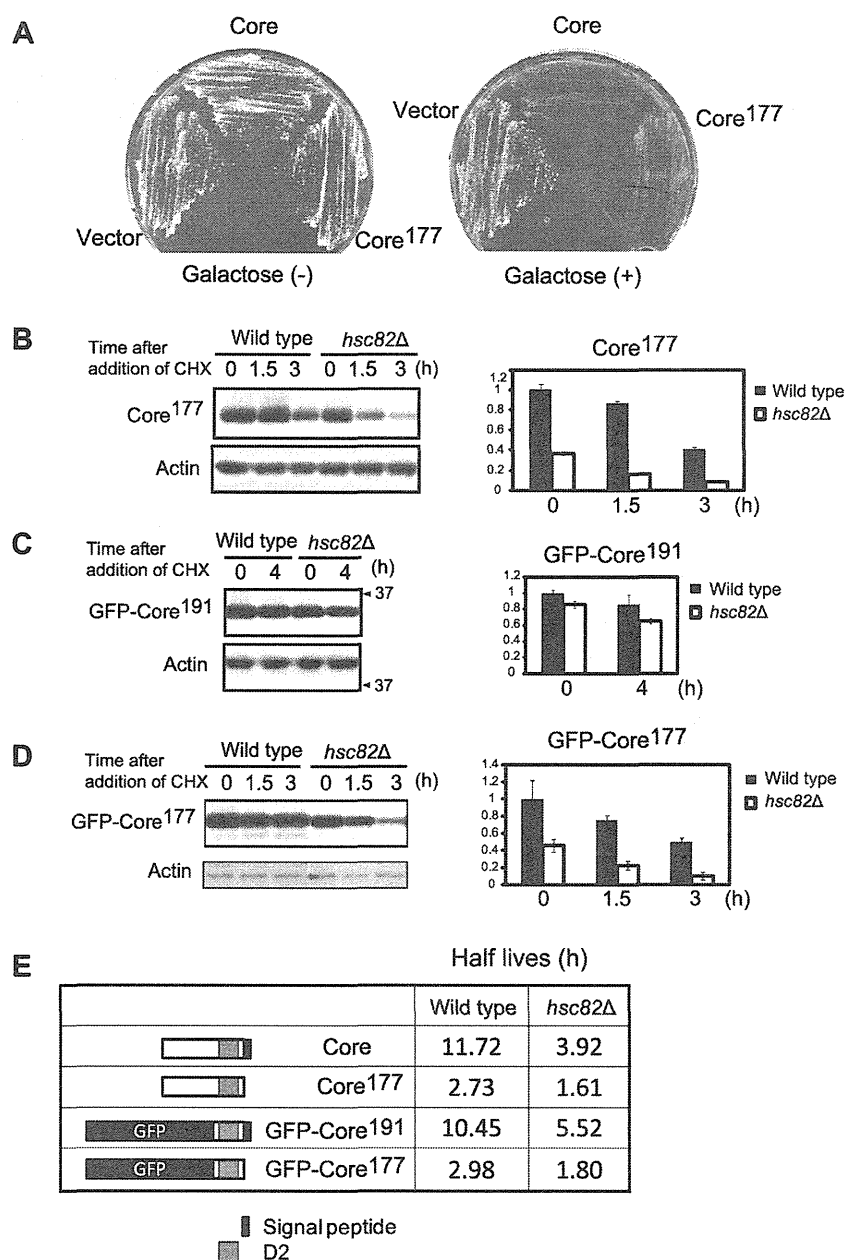


Fig. 5. The stability of the organelle association domain (D2 domain) of the Core depends on HSP90 activity. (A) Effect of yeast cell growth by Core¹⁷⁷ was examined as described in legend to Fig. 1. (B–D) The stability of Core¹⁷⁷ (B), GFP fused to the D2 domain with the signal peptide (C) and the GFP fused to the D2 domain (D) were all lower in *hsc82Δ* cells. Log-phase cultures of wild-type and *hsc82Δ* cells each harboring the corresponding plasmids were cultured with galactose for 2 h and then chased after treatment with CHX, as in Fig. 4. (E) Half-lives of Core, Core¹⁷⁷, GFP-Core¹⁹¹ and GFP-Core¹⁷⁷ in wild-type and *hsc82Δ* cells. The half-lives were determined in chase experiments (Figs. 4 and 5B–D).

previous results involving expression profiling of yeast suggest that Core induces the expression of genes involved in the ER stress response, but not the heat stress response that induces molecular chaperons [22]. Furthermore, Core did not increase the level of a heat-inducible HSP90 (Hsp82; Fig. 3E). Thus, Core and Core¹⁷⁷ expressed in the yeast cells may fold correctly, accumulate on the ER, and induce cellular responses involved in the observed growth inhibition. Growth of yeast cells were not significantly affected by GFP-fused D2 peptides (GFP-Core¹⁹¹ and GFP-Core¹⁷⁷; data not shown). Consequently, it is possible that some characteristics of N-terminal region such as oligomerization [4] also may impact

on the yeast cell growth. Several reports indicate that expression of Core disturbs cellular signaling and enhances the cell growth [23,24]. It is possible that higher level of Core expression in yeast cells inhibits intrinsic functions of ER (manuscript in preparation).

We showed that treatment with HSP90 inhibitors and disruption of *HSC82* reduced the stability of the nascent Core protein, but pre-existing Core protein was not affected by HSP90 inhibitors. Steady-state HSP90 family protein levels, which derive from the *HSC82* gene, could determine the stability (amount) of the Core, causing growth inhibition in yeast cells. We also demonstrated that the stability of nascent Core and Core¹⁷⁷ were increased in

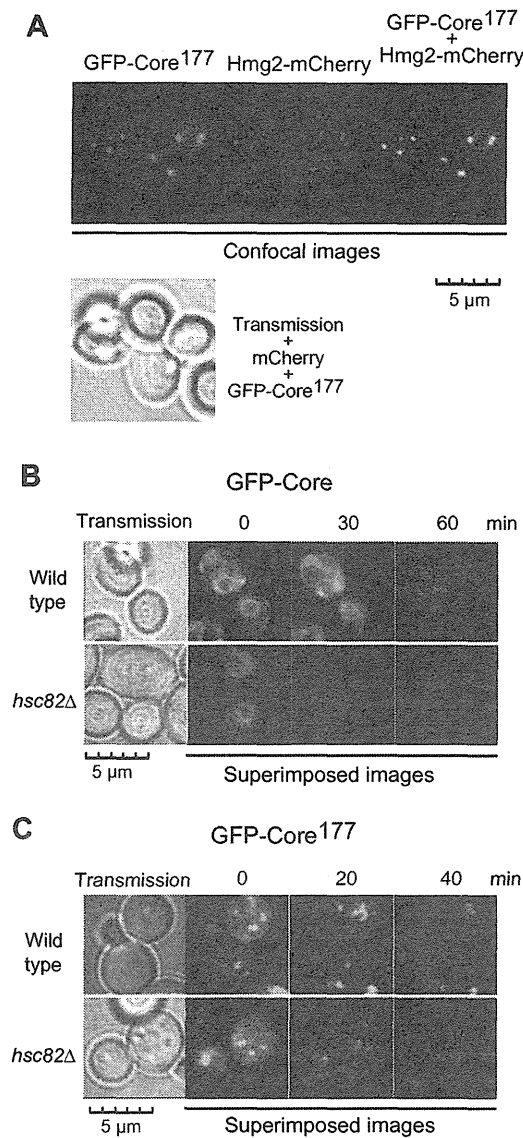


Fig. 6. Requirement of Hsc82 for ER localization of Core D2 region in yeast. (A) The GFP-Core¹⁷⁷ co-localized with the ER marker Hmg2-mCherry. Confocal images were monitored as described in legend to Fig. 1. Co-localization of GFP and mCherry and the transmission overlay are shown. (B and C) Hsc82 is required for extended Core localization to the ER. We monitored the time-dependent extinction of GFP-Core¹⁹¹ (0, 30, 60 min; B) and GFP-Core¹⁷⁷ (0, 20, 40 min; C) expressed in wild-type (upper panels) and *hsc82Δ* (lower panels) cells after production of GFP-Core proteins was stopped by switching from galactose to glucose in the medium (time 0). We acquired a series of 20 GFP images (0.26 μm Z dimension) and overlaid them (superimposed images).

an Hsc82-dependent manner and that the half-lives of GFP-fused D2 peptides (GFP-Core, GFP-Core¹⁷⁷) were comparable to those of Core and Core¹⁷⁷ (Fig. 5E). Our results suggest that Hsc82 activity might play a role in ensuring that the D2 peptide folds correctly, allowing the Core and Core¹⁷⁷ to be stabilized. Our results are consistent with the finding that the D2 domain is essential for the stability of the mature Core (Core¹⁷⁷), conferring protection from degradation in mammalian cells [5]. We failed to detect a direct interaction between Core and Hsp82/Hsc82 in yeast cells using immunoprecipitation (data not shown). Further studies are required to elucidate the Hsc82-dependent mechanism involved in

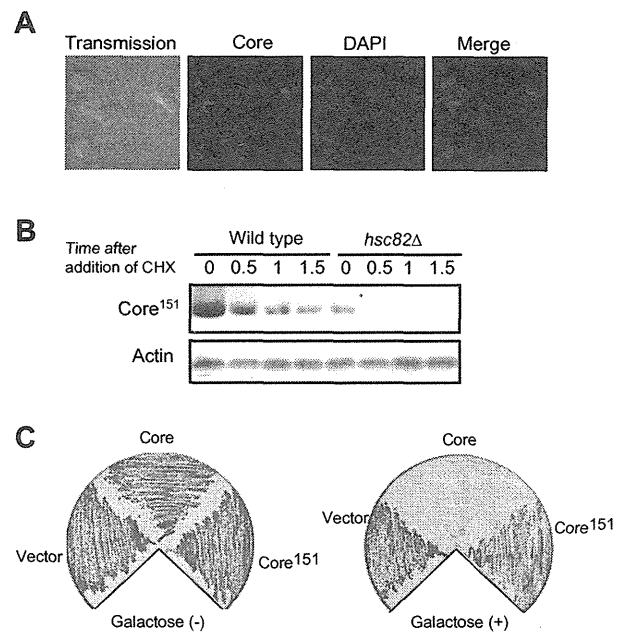


Fig. 7. ER localization and stability of Core¹⁵¹. (A) Localization of Core¹⁵¹ was examined as described in legend to Fig. 1. (B) The stability of Core¹⁵¹ was examined as described in legend to Fig. 5. (C) Growth of yeast cells carrying pRS425-GAL1-core (1b, aa 1–151) (Core¹⁵¹) were examined as described in legend to Fig. 1.

stabilization of the Core peptide chain during translation, including the potential requirement for a co-chaperone. In this aspect, one of the Hsp70 co-chaperon Ydj1 may be such a candidate: Ydj1 can interact with HSP90-client proteins [25] and protect nascent chains against degradation [26].

Thus far, we have no direct evidence of the effect of HSC90 on the stability of the D2 domain of Core in human hepatoma Huh7 cells. It is possible that the result demonstrated here may be specific to yeast cells. Nevertheless, the D2 domain is shown to be responsible for stability of Core in mammalian cells [27], thereby the yeast system presented herein, which can be applied to high-throughput screening, may be useful for identifying (screening or validation) for compounds that can direct the nascent D2 peptide to reduce the stability of the Core. Such compounds may represent possible drug candidates for prevention of the progression of HCV pathogenesis and HCV production.

Acknowledgments

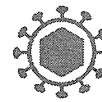
This study was supported by the “Program for Promotion of Fundamental Studies in Health Sciences” of the National Institute of Biomedical Innovation (NIBIO) and by Grants-in-Aid for Exploratory Research and a Grant-in-Aid for Scientific Research on Priority Areas (Life of Protein) from the Ministry of Education, Culture, Sports, Science and Technology of Japan. The authors thank Dr. T. Wakita (National Institute of Infectious Diseases) for providing the JFH1 cDNA clone and Dr. T.K. Nemoto (Nagasaki University) for providing the HSP90-specific antibody.

Appendix A. Supplementary data

Supplementary data associated with this article can be found, in the online version, at <http://dx.doi.org/10.1016/j.febslet.2012.05.023>.

References

- [1] Saito, I. et al. (1990) Hepatitis C virus infection is associated with the development of hepatocellular carcinoma. *Proc. Natl. Acad. Sci. USA* 87, 6547–6549.
- [2] Poynard, T., Yuen, M.F., Ratziu, V. and Lai, C.L. (2003) Viral hepatitis C. *Lancet* 362, 2095–2100.
- [3] Bartenschlager, R., Frese, M. and Pietschmann, T. (2004) Novel insights into hepatitis C virus replication and persistence. *Adv. Virus Res.* 63, 71–180.
- [4] McLauchlan, J. (2000) Properties of the hepatitis C virus core protein: a structural protein that modulates cellular processes. *J. Viral Hepat.* 7, 2–14.
- [5] McLauchlan, J., Lemberg, M.K., Hope, G. and Martoglio, B. (2002) Intramembrane proteolysis promotes trafficking of hepatitis C virus core protein to lipid droplets. *EMBO J.* 21, 3980–3988.
- [6] Targett-Adams, P., Hope, G., Boulant, S. and McLauchlan, J. (2008) Maturation of hepatitis C virus core protein by signal peptide peptidase is required for virus production. *J. Biol. Chem.* 283, 16850–16859.
- [7] Rouille, Y. et al. (2006) Subcellular localization of hepatitis C virus structural proteins in a cell culture system that efficiently replicates the virus. *J. Virol.* 80, 2832–2841.
- [8] Negro, F. (2006) Mechanisms and significance of liver steatosis in hepatitis C virus infection. *World J. Gastroenterol.* 12, 6756–6765.
- [9] McLauchlan, J. (2009) Hepatitis C virus: viral proteins on the move. *Biochem. Soc. Trans.* 37, 986–990.
- [10] Dunn, B. and Wobbe, C.R. (1997) *Saccharomyces cerevisiae* in: Current Protocols in Molecular Biology (Ausubel, R., Brent, R., Kingston, R.E., Moore, D.D., Seidman, J.G., Smith, J.A. and Struhl, K., Eds.), John Wiley & Sons, Inc., New York, pp. 13.1.1–13.1.3.
- [11] Christianson, T.W., Sikorski, R.S., Dante, M., Shero, J.H. and Hieter, P. (1992) Multifunctional yeast high-copy-number shuttle vectors. *Gene* 110, 119–122.
- [12] Okazaki, S., Tachibana, T., Naganuma, A., Mano, N. and Kuge, S. (2007) Multistep disulfide bond formation in Yap1 is required for sensing and transduction of H₂O₂ stress signal. *Mol. Cell* 27, 675–688.
- [13] Kawano, T. et al. (2004) A comprehensive study on the immunological reactivity of the Hsp90 molecular chaperone. *J. Biochem.* 136, 711–722.
- [14] Kishimoto, J., Fukuma, Y., Mizuno, A. and Nemoto, T.K. (2005) Identification of the pentapeptide constituting a dominant epitope common to all eukaryotic heat shock protein 90 molecular chaperones. *Cell Stress Chaperones* 10, 296–311.
- [15] Kashiwakuma, T. et al. (1996) Detection of hepatitis C virus specific core protein in serum of patients by a sensitive fluorescence enzyme immunoassay (FEIA). *J. Immunol. Methods* 190, 79–89.
- [16] Ferrigno, P. and Silver, P.A. (1999) Analysis of nuclear transport in vivo. *Methods Cell Biol.* 58, 107–122.
- [17] Okamoto, K. et al. (2008) Intramembrane processing by signal peptide peptidase regulates the membrane localization of hepatitis C virus core protein and viral propagation. *J. Virol.* 82, 8349–8361.
- [18] Hampton, R.Y., Koning, A., Wright, R. and Rine, J. (1996) In vivo examination of membrane protein localization and degradation with green fluorescent protein. *Proc. Natl. Acad. Sci. USA* 93, 828–833.
- [19] Prodromou, C. and Pearl, L.H. (2003) Structure and functional relationships of Hsp90. *Curr. Cancer Drug Targets* 3, 301–323.
- [20] Taipale, M., Jarosz, D.F. and Lindquist, S. (2010) HSP90 at the hub of protein homeostasis: emerging mechanistic insights. *Nat. Rev. Mol. Cell Biol.* 11, 515–528.
- [21] Borkovich, K.A., Farrelly, F.W., Finkelstein, D.B., Taulien, J. and Lindquist, S. (1989) Hsp82 is an essential protein that is required in higher concentrations for growth of cells at higher temperatures. *Mol. Cell Biol.* 9, 3919–3930.
- [22] Kubota, N., Naganuma, A. and Kuge, S. (2007) DNA microarray analysis of transcriptional responses of yeast cells to expression of core protein of hepatitis C virus. *J. Toxicol. Sci.* 32, 201–204.
- [23] Sato, Y. et al. (2006) Hepatitis C virus core protein promotes proliferation of human hepatoma cells through enhancement of transforming growth factor α expression via activation of nuclear factor- κ B. *Gut* 55, 1801–1808.
- [24] Cho, J.W., Baek, W.K., Suh, S.I., Yang, S.H., Chang, J., Sung, Y.C. and Suh, M.H. (2001) Hepatitis C virus core protein promotes cell proliferation through the upregulation of cyclin E expression levels. *Liver* 21, 137–142.
- [25] Flom, G.A., Lemieszek, M., Fortunato, E.A. and Johnson, J.L. (2008) Farnesylation of Ydj1 is required for in vivo interaction with Hsp90 client proteins. *Mol. Biol. Cell* 19, 5249–5258.
- [26] Mandal, A.K., Nillegoda, N.B., Chen, J.A. and Caplan, A.J. (2008) Ydj1 protects nascent protein kinases from degradation and controls the rate of their maturation. *Mol. Cell Biol.* 28, 4434–4444.
- [27] Hope, R.G. and McLauchlan, J. (2000) Sequence motifs required for lipid droplet association and protein stability are unique to the hepatitis C virus core protein. *J. Gen. Virol.* 81, 1913–1925.



RESEARCH

Open Access

PA from an H5N1 highly pathogenic avian influenza virus activates viral transcription and replication and induces apoptosis and interferon expression at an early stage of infection

Qiang Wang^{1,2†}, Shijian Zhang^{2,3,4†}, Hongbing Jiang², Jinlan Wang², Leiyun Weng², Yingying Mao², Satoshi Sekiguchi⁵, Fumihiko Yasui⁵, Michinori Kohara⁵, Philippe Buchy⁶, Vincent Deubel⁶, Ke Xu¹, Bing Sun¹ and Tetsuya Toyoda^{2,5,7*}

Abstract

Background: Although gene exchange is not likely to occur freely, reassortment between the H5N1 highly pathogenic avian influenza virus (HPAIV) and currently circulating human viruses is a serious concern. The PA polymerase subunit of H5N1 HPAIV was recently reported to activate the influenza replicon activity.

Methods: The replicon activities of PR8 and WSN strains (H1N1) of influenza containing PA from HPAIV A/Cambodia/P0322095/2005 (H5N1) and the activity of the chimeric RNA polymerase were analyzed. A reassortant WSN virus containing the H5N1 Cambodia PA (C-PA) was then reconstituted and its growth in cells and pathogenicity in mice examined. The interferon promoter, TUNEL, and caspase 3, 8, and 9 activities of C-PA-infected cells were compared with those of WSN-infected cells.

Results: The activity of the chimeric RNA polymerase was slightly higher than that of WSN, and C-PA replicated better than WSN in cells. However, the multi-step growth of C-PA and its pathogenicity in mice were lower than those of WSN. The interferon promoter, TUNEL, and caspase 3, 8, and 9 activities were strongly induced in early infection in C-PA-infected cells but not in WSN-infected cells.

Conclusions: Apoptosis and interferon were strongly induced early in C-PA infection, which protected the uninfected cells from expansion of viral infection. In this case, these classical host-virus interactions contributed to the attenuation of this strongly replicating virus.

Keywords: Influenza virus, PA, Transcription, Replication, Apoptosis, Interferon

* Correspondence: toyoda_tetsuya@yahoo.co.jp

†Equal contributors

²Units of Viral Genome Regulation, the Key Laboratory of Molecular Virology & Immunology, Institut Pasteur of Shanghai, Chinese Academy of Sciences, 411 Hefei Road, 200025, Shanghai, P. R. China

⁵Department of Microbiology and Cell Biology, Tokyo Metropolitan Institute of Medical Biology, 3-18-22 Honkomagome, Bunkyo-Ku, Tokyo 113-8613, Japan

Full list of author information is available at the end of the article



Background

Influenza A viruses cause disease in humans, pigs, other mammals, and birds [1]. The genomes of influenza A viruses are composed of 8 negative-sense single-stranded RNA segments; this segmented genome allows gene reassortment between viruses in co-infected cells to produce new viruses. Reassortment of influenza A virus genes caused the deadly H2N2 “Asian flu” and the H3N2 “Hong Kong flu” pandemics in 1957 and 1968, respectively. During these pandemics, the avian virus PB1, HA and NA, or PB1 and HA genes, respectively, were introduced into circulating human viruses [2,3]. The last pandemic strain, the novel swine-origin influenza virus A/H1N1 (S-OIV), carries PB2 and PA genes of avian origin [4]. In addition to the S-OIV pandemic flu, H5N1 highly pathogenic avian influenza viruses (HPAIV) have caused severe or fatal disease in humans in Asia, the Middle East, and Africa since their emergence in Hong Kong in 1997 (WHO, http://www.who.int/csr/disease/avian_influenza/en/). The H5N1 influenza virus ribonucleoprotein complex (RNP) contributes to viral pathogenesis in chickens [5,6]. Influenza viruses with high polymerase activity have also shown high pathogenicity [7,8]. These lines of evidence suggest that the influenza RNA-dependent RNA polymerase (RdRp) contributes to its pathogenesis.

Influenza A virions contain 8 negative-sense single-stranded RNA genome segments and RdRp [9]. Genome segments 1, 2, and 3 encode the RdRp subunits PB2, PB1, and PA, respectively. Segment 4 encodes hemagglutinin (HA), segment 5 nucleoprotein (NP), segment 6 neuraminidase (NA), segment 7 matrix protein 1 (M1) and an ion channel (M2), and segment 8 non-structural protein 1 (NS1) and nuclear export protein (NEP). A second open reading frame of segment 2 encodes PB1-F2 in some strains.

The RdRp subunit PB1 is the core subunit of the RdRp complex and mediates RNA polymerization [10-12], while PB2 is the cap-binding subunit [13-15] and PA has cap-dependent endonuclease activity [16-20]. Influenza virus RdRp catalyzes both transcription of viral mRNA and replication of the viral genome. Influenza transcription is a prototype of primer-dependent initiation. The viral RdRp binds to the cap-1 structures of host mRNAs and cleaves off 9 to 15 nucleotides to generate primers for viral transcription, a process known as “cap snatching” [13,21-23]. The internal initiation mechanism of influenza virus genome replication was recently elucidated [24,25].

H5N1 HPAIV does not efficiently adapt to transmission to humans [26]. However, once it does infect humans, it results in high mortality of approximately 60% [27,28]. Although some genomic combinations, such as those between human H3N2, avian H5N1, and horse H7N7 or between human H3N2 and avian H2N2,

may be incompatible [29-32], reassortment between H5N1 HPAIV, which is epizootic among poultry almost worldwide [33], and currently circulating human influenza viruses, including the pandemic S-OIV and seasonal influenza viruses (H1N1 and H3N2), is one of the most important potential threats for the next pandemic. Kashiwagi *et al.* recently reported that the PA of H5N1 HPAIV activated the polymerase activity by enhancing promoter binding [34]. Multiple functions of PA in addition to promoter binding, such as transcription and replication [9,18], endonuclease activity [16,17,19,20,35], cap binding [19], protease activity [36], proteolysis induction [37], pathogenesis in mice [38], and thermal sensitivity of RNP [39], have been identified.

In this paper, we describe the activation of the polymerase activity of A/Puerto Rico/8/1934 (PR8, H1N1) and A/WSN/1933 (WSN, H1N1) RNPs by the H5N1 HPAIV PA of A/Cambodia/P0322095/2005, which was isolated from a Cambodian victim [40], and the reconstitution of the chimeric virus to analyze the effect of this H5N1 PA in the background of WSN, a well-studied mouse influenza infection model. We found a discrepancy between the viral polymerase activity and proliferation efficiency in cells and its pathogenesis in mice. We then analyzed the mechanism of the attenuation and the low pathogenicity of WSN carrying H5N1 PA.

Results

Effect of H5N1 Cambodia PA on the PR8 and WSN replicons and *in vitro* RdRp activity

We first examined the replicon activity in 293 T cells of a chimeric PR8 RNP containing H5N1 Cambodia PA (Figure 1A). Influenza replicon activity was measured as previously described [41,42]. The replicon activity was about $200.0 \pm 8.2\%$ that of the PR8 RNP (Student's *t*; $p < 0.005$), while the Cambodia RNP showed $43.8 \pm 2.9\%$ of the replicon activity of the PR8 RNP ($p < 0.005$). The expression of RdRp and NP in the transfected cells was confirmed by western blotting (Additional file: Figure S1).

As we found 2-fold activation of the PR8 replicon by H5N1 Cambodia PA, we purified both PR8 RdRp and a chimeric RdRp (PR8PB2-PR8PB1-H5N1 Cambodia PA) in order to investigate the effect of the H5N1 Cambodia PA on RdRp activity *in vitro*. Sodium dodecyl sulfate-polyacrylamide gel electrophoresis (SDS-PAGE) showed that H5N1 Cambodia PA migrated to a higher position than did PR8PA; the Cambodia PA band almost overlapped with that of $18 \times$ HisPR8PB2 (Figure 1B). The identity of H5N1 Cambodia PA was confirmed by western blotting against PA (Figure 1C).

We next compared the activities of the purified RdRps *in vitro*. We tested the transcription activity using v84 and globin mRNA primers (Figure 1D and E, mRNA), and replication activity using v84 and c84 with and

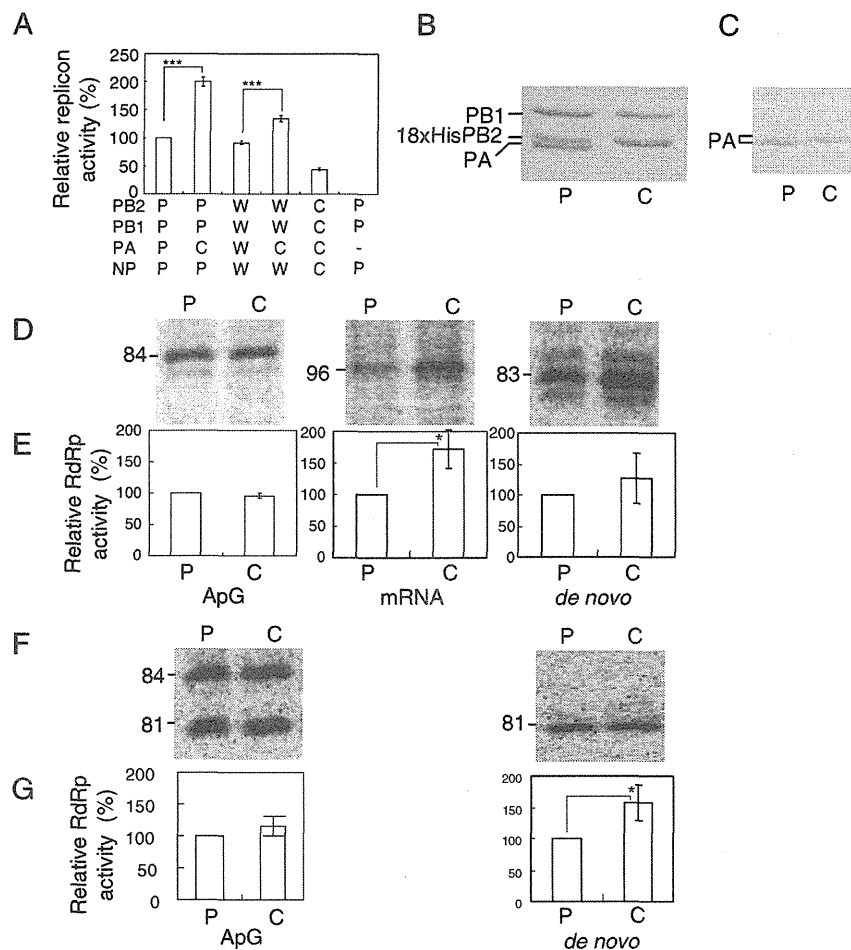


Figure 1 Replicon and *in vitro* RNA-dependent RNA polymerase (RdRp) activities of the chimeras of H5N1 Cambodia PA with PR8 and WSN. **A:** Replicon activity of the chimeric influenza virus ribonucleoproteins (RNPs) of WSN and PR8 with H5N1 Cambodia PA. The relative replicon activities of WSN and PR8 with H5N1 Cambodia PA in 293 T cells were compared with those of WSN and PR8. The combination of PB2, PB1, PA, and NP is indicated below the graph. W, WSN; P, PR8; C, H5N1 Cambodia. As a negative control, PR8 replicon without PA was used. **B:** Purified influenza virus PR8 RdRp (P) and PR8PB2-PR8PB1-C-PA RdRp (C). Each RdRp (5 pmol) was subjected to sodium dodecyl sulfate-polyacrylamide gel electrophoresis (SDS-PAGE) on 7.5% gels and Coomassie brilliant blue staining. The positions of PB1, 18 × His-PB2, and PA are indicated on the left. **C:** Western blot of the purified influenza virus chimeric RdRp. Each RdRp (5 pmol) was electro-blotted onto the nitrocellulose membrane. The PA was detected by western blotting with anti-PA antibodies. The position of PA is indicated on the left. **D and E:** Comparison of the chimeric RdRp activities in *in vitro* transcription and replication of v84 with those of PR8. The v84 model template RNA (200 nM) was transcribed by PR8RdRp (P) or PR8PB2-PR8PB1-C-PA RdRp (C) with or without (*de novo*) 0.1 mM ApG (ApG) or 0.5 μg globin mRNA (mRNA). **F and G:** Comparison of chimeric RdRp activity in *in vitro* replication of c84 with that of PR8. The c84 model template RNA was incubated with or without ApG (*de novo*). Products were analyzed by PAGE on 6% gels containing 8 M urea and the images analyzed with a Typhoon Trio plus. Examples of the images are shown in D and F. The size of the product RNA is indicated on the left. The mean and standard deviation (error bar in the graph) of the polymerase activity relative to that of PR8 RdRp were calculated from 2 independent measurements of 3 different RdRp preparations. Statistical significance was evaluated with Student's *t*-test. **p* < 0.05, ****p* < 0.005.

without the dinucleotide primer ApG (Figure 1D, E, F, and G). ApG-primed and *de novo* initiation of v84 transcription produced 84- and 83-nt products, respectively, while globin mRNA-primed transcription produced 96-nt products. Because virion RdRp uses 10–15 nucleotide primers to initiate from the C at the 2nd position from the 3' end of the genome [18,22], the 96-mer products

were assigned to the transcripts from the 13th G next to the 12th U of the cap-1 structure (m⁷GmACACUUCUUUU) of rabbit β-globin mRNA (GenBank; M10843). The mean and standard deviation (error bar in the graph) of the polymerase activity relative to that of PR8 RdRp were calculated from 2 independent measurements of 3 different RdRp preparations. The relative

ApG-primed replication activity of the chimeric RdRp was $95.9 \pm 4.5\%$ of that of PR8 RdRp, while its *de novo* replication activity was $126 \pm 40\%$ of that of PR8 RdRp. The chimeric RdRp produced $171 \pm 31\%$ ($p < 0.05$) of the amount of 96-nt transcription products. ApG-primed initiation of c84 produced 84- and 81-nt products, while *de novo* initiation produced 81-nt products. The relative replication activity of ApG-primed initiation of c84 by the chimeric RdRp was $116 \pm 16\%$ of that by PR8 RdRp, while its *de novo* initiation was $156 \pm 29\%$ of that by PR8 RdRp ($p < 0.05$). We thus confirmed that H5N1 Cambodia PA enhanced both the transcription and replication activities of PR8 RdRp.

Before reconstituting WSN carrying H5N1 Cambodia PA, we tested the effect of H5N1 Cambodia PA on the WSN replicon (Figure 1A). WSN replicon activity ($91.3 \pm 3.2\%$) was similar to that of PR8. The replicon activity of WSN containing the H5N1 Cambodia PA (which was $133.9 \pm 5.8\%$ of that of the PR8 replicon) was about 1.5-fold higher than that of the WSN replicon ($p < 0.005$). Therefore, we also observed an activation effect of H5N1 Cambodia PA on the WSN replicon.

Effect of H5N1 Cambodia PA on virus growth in MDCK cells, chicken embryo fibroblasts (CEF), and Vero cells

Next, we tested whether the RdRp activation effect of H5N1 Cambodia PA affected virus growth. As the RdRp

subunits of PR8 and WSN are highly homologous, with 96, 97, and 98% amino acid identity between the PB2, PB1, and PA genes, respectively, and as the activation effect of H5N1 Cambodia PA was confirmed in both the WSN and PR8 replicons, we used a WSN reconstitution system to analyze the effect of H5N1 Cambodia PA in H1N1 virus. The WSN virus carrying H5N1 Cambodia PA (C-PA) was reconstituted successfully. First, we compared the multi-step growth of C-PA with that of WSN in MDCK, CEF, and Vero cells.

In MDCK cells, the C-PA titer was always lower than that of WSN and plateaued ($4.7 \pm 0.2 \times 10^4$ PFU/mL) 16 hr post-infection (pi), while the WSN titer was $2.2 \pm 0.03 \times 10^5$ PFU/mL 16 hr pi and plateaued ($5.6 \pm 1.6 \times 10^6$ PFU/mL) 36 hr pi (Figure 2A). The C-PA titer in MDCK cells 60 hr pi was significantly higher than that of WSN ($p < 0.001$). The titers of C-PA and WSN in CEF did not plateau even 60 hr pi. However, the C-PA titer 60 hr pi ($7.1 \pm 1.4 \times 10^5$ PFU/mL) was about half of that of WSN ($1.3 \pm 0.4 \times 10^6$ PFU/mL), a statistically significant difference ($p < 0.001$, Figure 2B). We therefore observed a discrepancy between the effects of H5N1 Cambodia PA on RdRp activity and on virus growth in MDCK and CEF cells. However, the C-PA titer in Vero cells between 24 hr and 60 hr pi was significantly higher than that of WSN ($p < 0.05$, Figure 2C). Both titers plateaued at $5.6 \pm 0.1 \times 10^5$ PFU/mL 70 hr pi.

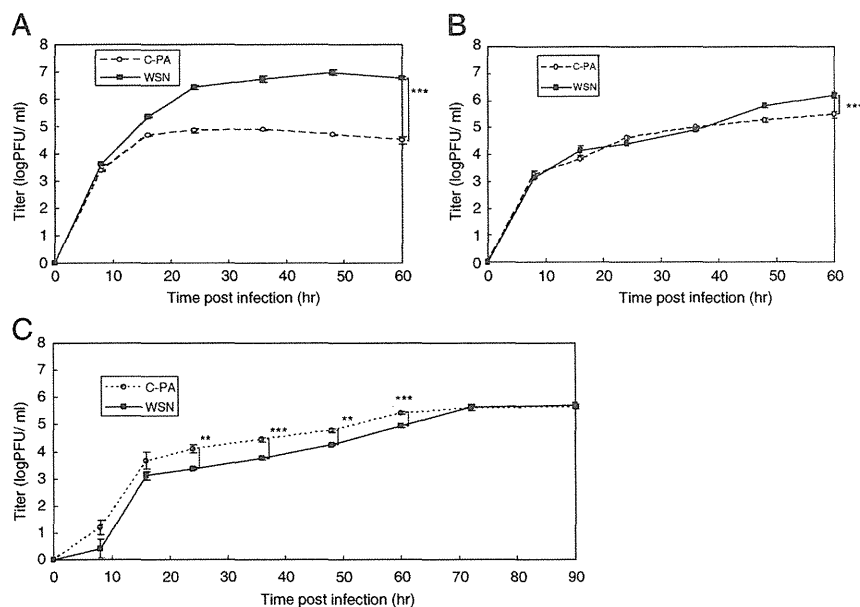


Figure 2 Multi-step growth curves of C-PA and WSN in infected cells. MDCK (A), chicken embryo fibroblast (CEF) (B), and Vero (C) cells were infected with C-PA or WSN at a multiplicity of infection (MOI) of 0.01. Viruses were harvested 8, 16, 24, 36, 48, and 60 hr (additional 72 and 90 hr for Vero cells) after infection and their titers on MDCK cells measured by a plaque-formation assay. The mean and standard deviation (error bar in the graph) of each plaque titer were calculated from 3 independent experiments. Statistical significance was evaluated with Student's *t*-test.

** $p < 0.01$, *** $p < 0.005$.

No cytopathic effect was apparent in Vero cells (data not shown).

We next compared single-step growth of C-PA and WSN in MDCK and Vero cells (Figure 3). The C-PA titers in both MDCK and Vero cells between 4 and 12 hr pi were higher than those of WSN. The C-PA titer in MDCK cells 12 hr pi ($1.6 \pm 0.9 \times 10^6$ PFU/mL) was significantly higher than that of WSN ($1.3 \pm 0.7 \times 10^5$ PFU/mL) ($p < 0.005$, Figure 3A). The C-PA titer in Vero cells 12 hr pi ($1.6 \pm 0.9 \times 10^5$ PFU/mL) was significantly higher than that of WSN ($2.9 \pm 0.2 \times 10^4$ PFU/mL) ($p < 0.05$, Figure 3B). The growth of C-PA in both MDCK and Vero cells plateaued 6 hr pi. WSN growth in Vero cells plateaued 8 hr pi, while its titer in MDCK cells continued to increase up to 12 hr pi.

Pathogenicity of the C-PA virus in mice

We also examined the pathogenicity of C-PA in mice. The LD₅₀ for mouse nasal infection was calculated from

the survival rate of the infected mice by the method of Reed and Munch (Figure 4) [43]. The LD₅₀ values of C-PA and WSN were 5×10^5 PFU and 1×10^4 PFU, respectively. The pathogenicity of C-PA is therefore lower than that of WSN, despite its higher RdRp activity, both in cell culture (as reflected by the multi-step growth) and in mice.

We thus confirmed the discrepancy between the RdRp activity and pathogenicity both in cells (virus titer) and in mice. The genome sequence of the C-PA stock was confirmed to be identical to that of the genome reconstitution plasmids.

Interferon induction

Because the multi-step growth activity of C-PA was lower than that of WSN in MDCK and CEF cells but better in Vero cells, and because the single-step growth activity of C-PA was better than that of WSN in both MDCK and Vero cells, we examined the effect of C-PA

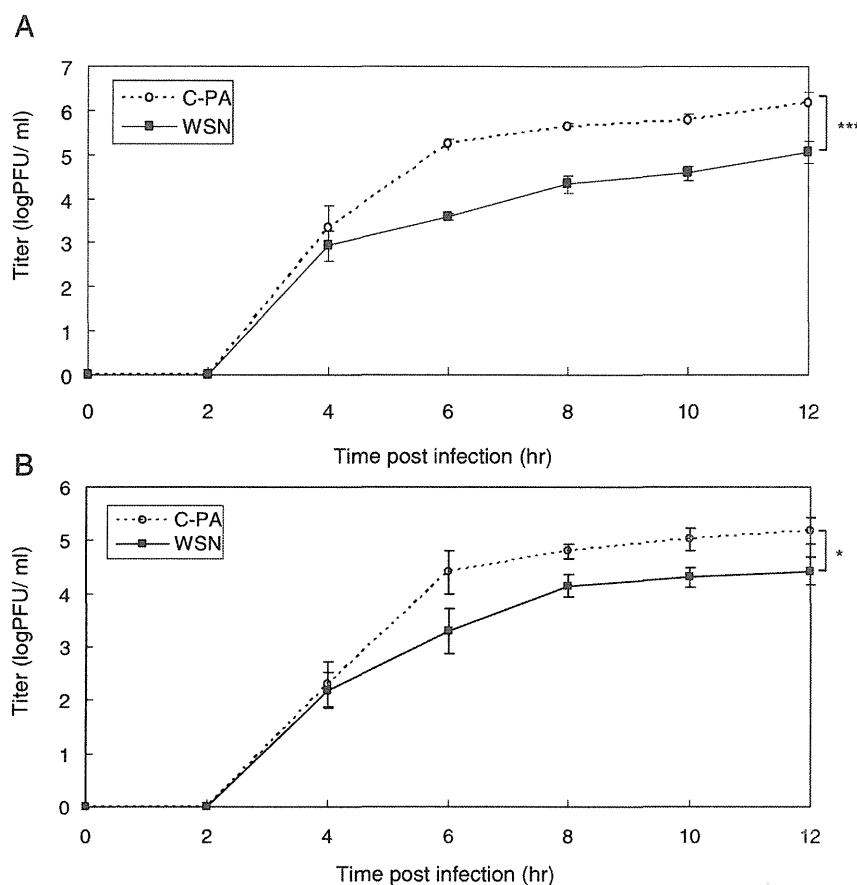
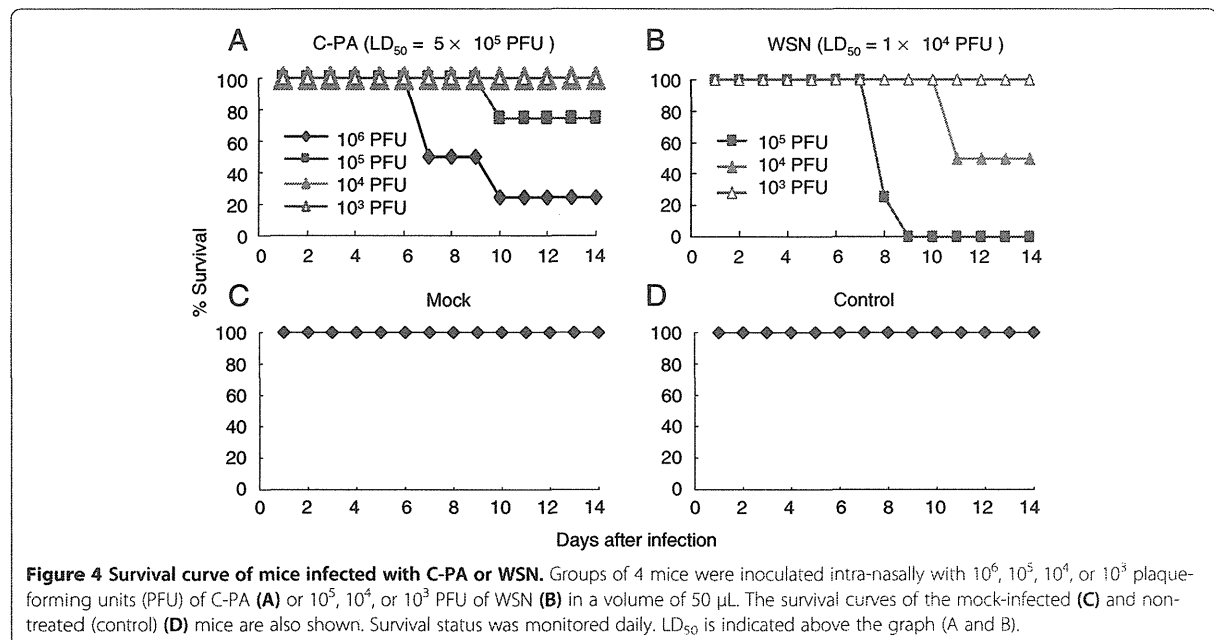


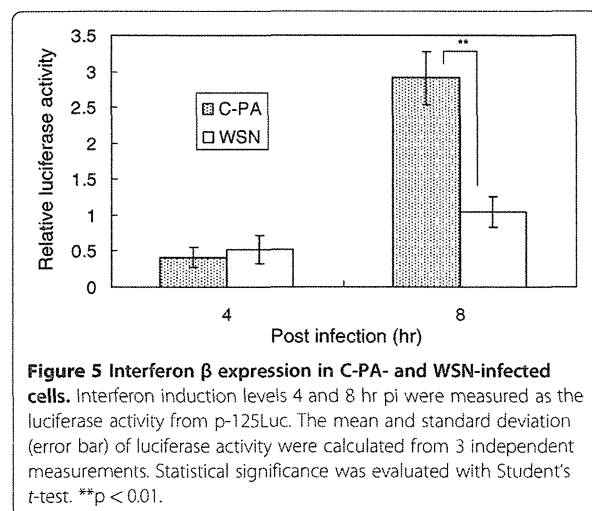
Figure 3 Single-step growth curves of C-PA and WSN in infected cells. MDCK (A) and Vero (B) cells were infected with C-PA or WSN at an MOI of 5. Viruses were harvested 2, 4, 6, 8, 10, and 12 hr after infection and their titers on MDCK cells measured by a plaque-formation assay. The mean and standard deviation (error bar in the graph) of each plaque titer were calculated from 3 independent experiments. Statistical significance was evaluated with Student's t-test. * $p < 0.05$, *** $p < 0.005$.



on the activity of the host cellular defense system. First, we examined interferon β induction in 293 T cells by measuring the activity of its promoter (Figure 5). A small amount of interferon β was induced in cells infected with either C-PA or WSN 4 hr pi. However, interferon β promoter activity was almost 3-fold higher ($p < 0.01$) in the C-PA-infected cells than in the WSN-infected cells 8 hr pi.

TUNEL assay

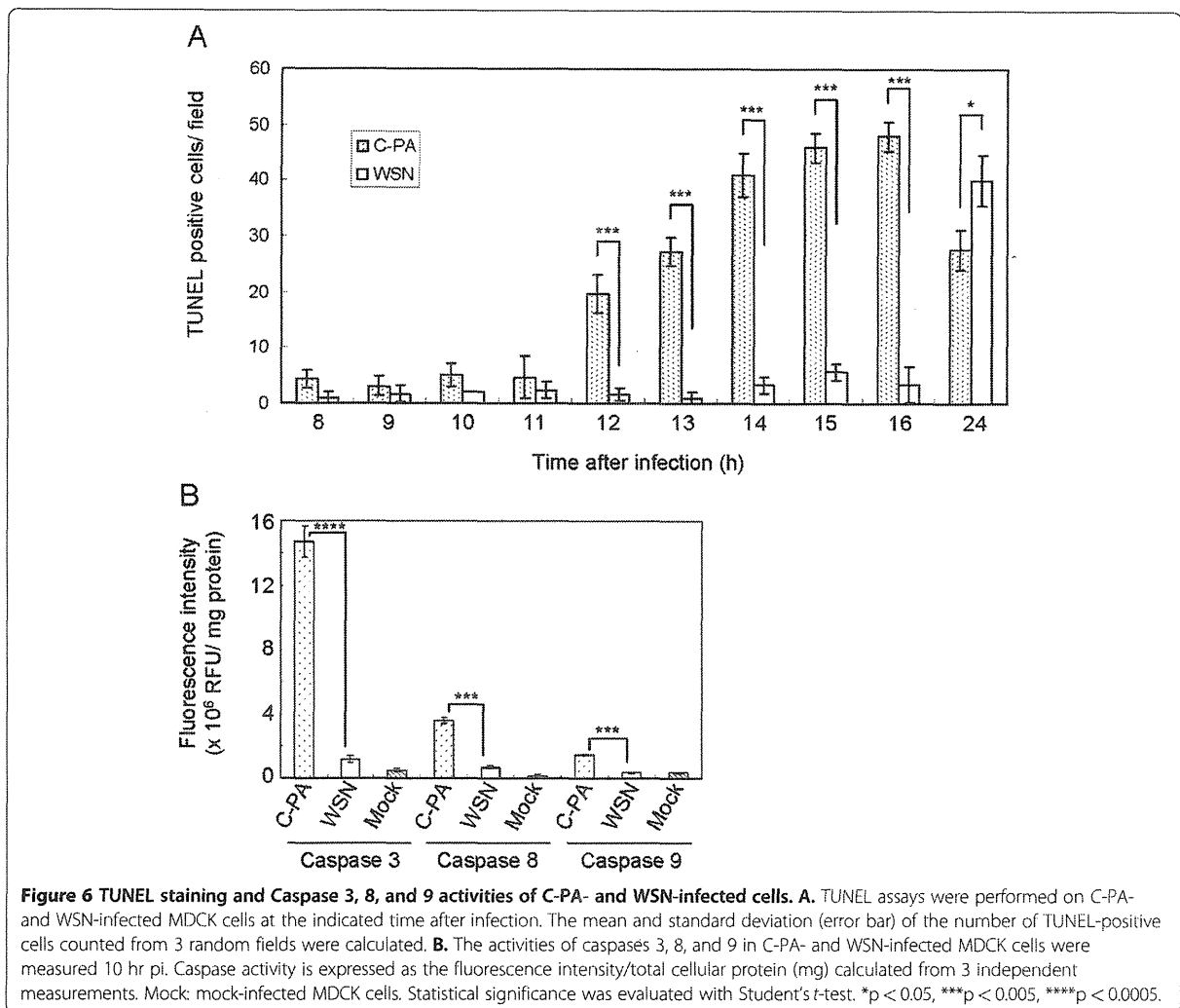
Next, we examined the induction of apoptosis in MDCK cells by performing TUNEL assays hourly from 8 to 16 hr pi and once more 24 hr pi. The numbers of



TUNEL-positive cells in 3 random fields were counted (Figure 6A). Before 11 hr pi, we found fewer than 5 TUNEL-positive cells per field in either C-PA- or WSN-infected cells. Then, beginning 12 hr pi, the numbers of the C-PA-infected TUNEL-positive cells increased to 20 ± 3.5 (12 hr), 27 ± 2.5 (13 hr), 41 ± 4.0 (14 hr), 46 ± 2.6 (15 hr), 48 ± 2.6 (16 hr), and 28 ± 3.5 (24 hr). The numbers of the WSN-infected TUNEL-positive cells remained less than 6 until 16 hr and then increased to 40 ± 4.6 at 24 hr pi. From 12 to 16 hr pi, significantly more TUNEL-positive cells were observed among the C-PA-infected cells than among the WSN-infected cells ($p < 0.005$). TUNEL-positive cells were clearly observed among both C-PA- and WSN-infected cells, and significantly more TUNEL-positive cells were observed among WSN-infected cells than among C-PA-infected cells 24 hr pi ($p < 0.05$). In conclusion, TUNEL-positive cells appeared earlier in C-PA-infected cells than in WSN-infected cells. No differences in TUNEL staining were found among cells transfected with WSN and H5N1 Cambodia single-protein-expression plasmids (PB2, PB1, PA, HA, NP, NA, M1, M2, NS1, and NS2) or pcDNA3.1 (data not shown).

Caspase 3, 8, and 9 activities

TUNEL-positive cells may be apoptotic. Caspases are central players in both the intrinsic and the extrinsic pathways of apoptosis [44-46]. We therefore measured the activities of caspases 3, 8, and 9 in C-PA- and WSN-infected cells 10 hr pi, 2 hr before TUNEL-positive cells could first be observed among C-PA-infected cells, in order to confirm



the induction of apoptosis (Figure 6B). The activities of caspases 3 ($14.7 \pm 9.8 \times 10^6$ RFU/mg protein, $p < 0.0005$), 8 ($3.6 \pm 0.2 \times 10^6$ RFU/mg protein, $p < 0.005$), and 9 ($1.5 \pm 0.5 \times 10^6$ RFU/mg protein, $p < 0.005$) were higher in C-PA-infected cells than in WSN-infected cells 10 hr pi (comparisons evaluated by Student's *t* test). The caspase activities in WSN-infected cells were similar to those in mock-infected cells, indicating that WSN infection did not induce apoptosis 10 hr pi. The activation of caspase 9 in C-PA-infected cells indicates that C-PA infection induces apoptosis through the mitochondrial pathway [47-49], and the apoptosis induction by C-PA began at an early time after infection at which no apoptosis was induced by WSN infection.

Histopathology and TUNEL assay of infected mice

Finally, we compared the pathological changes in the lung between C-PA- and WSN-infected mice. The

histopathological appearances were similar (Figure 7). The major difference between C-PA- and WSN-infected lungs is that pulmonary edema around blood vessels was present in the C-PA-infected lungs from day 1 pi, although it was also present in WSN-infected lungs on days 3 and 4 pi. On the first day of infection, a moderate amount of lymphocyte infiltration was observed around the bronchioles of C-PA-infected mouse lungs, and this inflammation decreased on days 3 and 4. More lymphocyte infiltration around the bronchioles was observed in WSN-infected mouse lungs on days 1-3, with the most severe inflammation on day 2, and only mild inflammation was observed on day 4. No pathological change was observed in the mock-infected or non-infected mouse lungs.

We simultaneously analyzed these samples by TUNEL assay. A few TUNEL-positive cells were observed in both C-PA- and WSN-infected mouse lungs on days 1-4 pi,

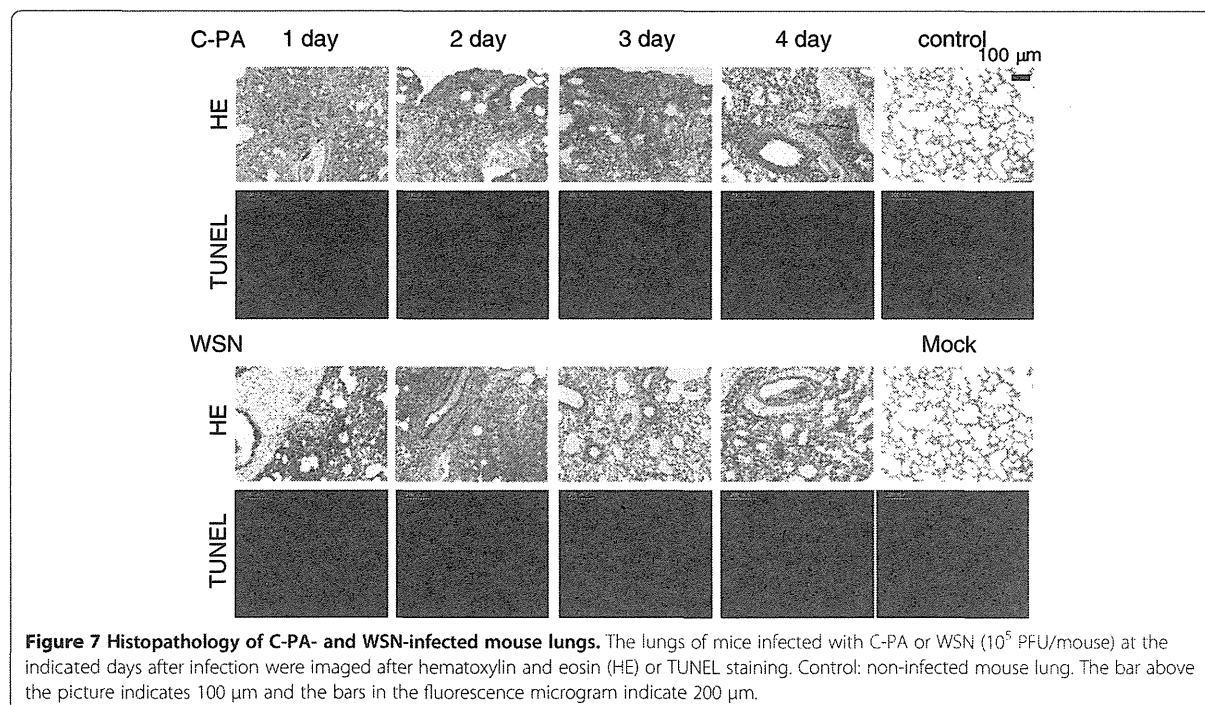


Figure 7 Histopathology of C-PA- and WSN-infected mouse lungs. The lungs of mice infected with C-PA or WSN (10^5 PFU/mouse) at the indicated days after infection were imaged after hematoxylin and eosin (HE) or TUNEL staining. Control: non-infected mouse lung. The bar above the picture indicates 100 µm and the bars in the fluorescence microgram indicate 200 µm.

but the numbers did not clearly differ between the 2 viruses. The histopathological findings indicated recovery of the C-PA-infected mouse lungs, which is consistent with the lower pathogenicity of C-PA.

Discussion

The activation of replicon activity by H5N1 HPAIV PA observed in this study has been reported several times (Figure 1) [34,50,51]. Influenza viruses with high polymerase activity have been reported to show high pathogenicity [7,8]. Therefore, reassortment of H5N1 HPAIV PA into human influenza viruses, including the seasonal influenza viruses (H1N1 and H3N2) and the pandemic influenza virus (H1N1), is a serious concern [34], although this event may not occur easily [32]. The major factor for host adaptation in H5N1 HPAIV RNP is PB2, which shows a strong correlation with pathogenicity in mammalian hosts, including humans [30,31,51-55].

The WSN reconstitution system [56] was used to analyze the effect of H5N1 Cambodia PA in an animal influenza virus (H1N1). Contrary to our expectation, the multi-step growth of C-PA in MDCK and CEF cells was less than that of WSN, and its pathogenicity was low because of this attenuation (Figures 2, 4). We confirmed the absence of mutations in the C-PA genome. As we previously found a similar discrepancy in influenza promoter/origin function due to a difference in activation of the host defense system [42], we examined whether the discrepancy between RdRp activity and pathogenicity

was also due to differences in host defense. As the multi-step growth of C-PA in Vero cells was better than that of WSN, and because its single-step growth, which is highly dependent on the polymerase activity, in both MDCK and Vero cells was better than that of WSN (Figure 3), we first examined the activity of the interferon β promoter and found that it was strongly activated (Figure 5) in CPA-infected cells.

Type I interferon is induced in virus-infected cells by a signal transduction pathway beginning with retinoic-acid-inducible gene-I (RIG-I), which recognizes 5'-triphosphate-containing influenza RNA [57-62]. In C-PA-infected cells, a large amount of vRNA was expressed from early stages of infection, which might more strongly trigger interferon induction (Figures 5 and Additional file: Figure S3) and thereby induce an antiviral state in uninfected cells that protected them from influenza infection (Additional file: Figure S2A) [63-65]. The better multi-step growth of C-PA relative to WSN in Vero cells, which are defective in type-I interferon production [66] (Figure 2C), and the better single-step growth of C-PA than of WSN (Figure 3), are consistent with the high *in vitro* polymerase activity and strong interferon induction in C-PA infected cells.

Apoptosis (programmed cell death) is another mechanism by which cells restrict viral infection including influenza [67]. However, virus-induced apoptosis causes tissue damage, which is one of the mechanisms of influenza pathogenicity [68]. Apoptosis also aids in the

release of influenza viruses [69,70]. WSN induced apoptosis in MDCK cells late in infection [71]. However, no apoptosis was induced by expression of any single protein of either WSN or H5N1 Cambodia. Apoptosis was strongly induced in C-PA-infected cells beginning early in infection when no apoptosis was induced in WSN-infected cells (Figure 6). The activation of caspase 9 indicated that this apoptosis was mediated through the mitochondrial pathway [72]. The increased expression of vRNA (Additional file: Figure S3) in C-PA infected cells due to the high replication activity promoted by H5N1 PA (Figure 1) induced both interferon and apoptosis, resulting in attenuation of C-PA proliferation (Figure 2). Neither caspase 3 nor 8 was induced by expression of WSN PA or Cambodia PA alone (data not shown). The strong induction of interferon discussed above also stimulates the induction of apoptosis *via* RNA-dependent protein kinase (PKR) [73]. Such rapid induction of apoptosis was also observed in duck cells infected with HPAIV [68]. However, in case of C-PA, early induction of apoptosis attenuated the proliferation of the virus and thus decreased its pathogenicity.

PB1-F2 is the only influenza virus protein that induces apoptosis in infected monocytes and potentiates apoptosis during infection [74-76]. The WSN PB1-F2 proteins of WSN and C-PA are identical. Kinetic analysis of viral RNAs (Additional file: Figure S3) indicates that PB1-F2 is unlikely to contribute to the strong induction of apoptosis in C-PA infected cells.

C-PA infection strongly induced both interferon production and apoptosis early in infection, which attenuated virus proliferation and pathogenicity despite high RdRp activity. This may be another reason, in addition to poor adaptation, for the difficulty of obtaining reassortant viruses carrying H5N1 HPAIV PA [31,32].

Methods

Cell culture

293 T and Vero cells were maintained in Dulbecco's modified Eagle minimal essential medium (DMEM) containing 10% fetal bovine serum (FBS). CEFs were prepared from 11-day-old embryonated chicken eggs by trypsin digestion and stored in liquid nitrogen. CEF and MDCK cells were maintained in DMEM containing 10% or 5% FBS, respectively.

Replicon assay

A standard replicon assay was performed as previously described [41,42,77]. Luciferase activity was measured using the Dual-Glo luciferase assay kit and a GloMax 96 Microplate Luminometer (Promega, Fitchburg, USA) after transfection of 0.1 μ g each of pCPB2, pCPB1, pCPA, pCNP, and ppoliNSluc and 0.01 μ g of pRL_{SV40} (Promega) using Lipofectamine 2000 (Invitrogen,

Carlsbad, USA). The PB2, PB1, PA, and NP genes of influenza A/Cambodia/P096/2005 (H5N1) [40] and A/WSN/33 (H1N1) [56] were PCR-amplified using specific oligonucleotides and cloned into pcDNA3.1(+) (Invitrogen), resulting in pcCamPB2wt, pcCamPB1, pcCamPA, pcCamNP, pcWSNPB2, pcWSNPB1, pcWSNPA, and pcWSNNP, respectively. Only data in which the variation of the Renilla luciferase activity was less than 3-fold variations were used. The oligonucleotide sequence information will be made available upon request.

Expression, purification, and *in vitro* transcription of the influenza virus RdRp

Expression, purification, and *in vitro* transcription of the influenza virus RdRp were performed as previously described [42,77,78]. Briefly, 100 nM influenza RdRp was incubated in 50 mM Tris-HCl (pH 8.0), 8 mM MgCl₂, 150 mM NaCl, 2 mM DTT, 0.5 mM ATP, 0.5 mM CTP, 0.5 mM GTP, 0.05 mM [α -³²P] UTP, 0.1 mM ApG or 0.01 mg/mL globin mRNA, 2000 U/mL RNase inhibitor, and 200 nM v84 and c84 model template RNA at 25 °C for 90 min. The product was analyzed by PAGE on 6% gels containing 8 M urea and the images analyzed with a Typhoon Trio plus (GE Healthcare, Bucks, UK).

Model RNA templates

v84 and c84 model RNA templates were prepared as previously reported [11].

Western blotting

Proteins were blotted onto nitrocellulose membranes (Millipore, Billerica, USA) by semi-dry electroblotting (Bio-Rad, Hercules, USA) after SDS-PAGE on 10% gels. The blotted membranes were blocked with 10% skim milk in 20 mM Tris-HCl (pH 7.5), 150 mM NaCl, and 0.02% Tween 20 (TBST), and western blotting was performed using rabbit anti-PB1, -PB2, -PA [11], and -PR8 (1:1,000 each) and anti-actin (1:100) antibodies as the primary antibodies. The membranes were then incubated with alkaline phosphatase-conjugated anti-rabbit IgG (1:7,500) or anti-mouse IgG (1:7,500), and the positions of the bound antibodies were visualized with nitroblue tetrazolium (NBT) and 5-bromo-4-chloro-3-indolyl phosphate (BCIP).

Reconstitution of influenza virus and plaque-formation assay

pHH21 and the influenza virus 12-plasmid reconstitution system of WSN were kindly provided by Dr. Hobom and Dr. Kawaoka [56]. The H5N1 A/Cambodia/P0322095/2005 [40] PA sequence was inserted into ppoli-WSN-PA, resulting in ppoli-Cam-PA. The influenza virus WSN strain (WSN) and WSN carrying H5N1

Cambodia PA (C-PA) were reconstituted by co-transfection of 293 T cells with ppoll-WSN-PB2, ppoll-WSN-PB1, ppoll-WSN-PA or ppoll-Cam-PA, ppoll-WSN-HA, ppoll-WSN-NP, ppoll-WSN-NA, ppoll-WSN-M, and ppoll-WSN-NS with pCPB2, pCPB1, pCPA, and pCNP [10,56] using Lipofectamine 2000. The reconstituted viruses were recovered from the culture media 72 hr post-transfection. The viruses were plaque-purified, amplified, and titered on MDCK cells by a plaque-formation assay and stored at -80°C . The genome sequences of all viruses were determined by RT-PCR. The primer sequences used will be made available upon request.

Virus growth assay

MDCK, CEF, and Vero cells in 3.5-cm dishes (21 dishes of MDCK cells and CEFs, 27 dishes of Vero cells per a virus) were infected with WSN and C-PA at an MOI of 0.01 at 37°C for 1 hr (multi-step growth assay). The cells were washed $3\times$ with phosphate-buffered saline (PBS) and incubated with 2 mL of DMEM containing 2% FBS (without trypsin) at 37°C , as WSN replicates without trypsin [79]. All of the supernatants of 3 dishes of each cell were taken 6, 12, 24, 36, 48, and 60 hr (and also at 72 and 90 hr for Vero cells) after infection and stored at -80°C . Virus growth was also tested in MDCK and Vero cells after infection at an MOI of 5 (single-step growth assay). Supernatants were harvested 2, 4, 6, 8, 10, and 12 hr after infection. The viruses in the supernatants were titered on MDCK cells by a plaque-formation assay.

Mouse infection

Groups of 4 6-week-old female BALB/c mice (Sino-British Laboratory Animal, Shanghai, China) were anesthetized with ether and inoculated with 10^5 , 10^4 , or 10^3 PFU of WSN or 10^6 , 10^5 , 10^4 , or 10^3 PFU of C-PA in a volume of 50 μL by nasal dropping. Four mice were inoculated with 50 μL of PBS as a mock-infection control. The survival rates were monitored daily and the 50% lethal doses (LD_{50} s) calculated [41].

Histopathological analysis

Six-week-old female BALB/c mice were anesthetized with ether and inoculated with 10^5 PFU of WSN or C-PA in 50 μL by nasal dropping. Mice were inoculated with 50 μL of PBS as a mock-infection control. A non-treated mouse was used as a non-treated control. The mock-infected and infected mice were sacrificed by cervical dislocation under anesthesia on days 1, 2, 3, and 4 after infection, and their lungs were removed and fixed with 3.5% formalin/PBS at 25°C for 2 days. The lungs were embedded in paraffin blocks, sectioned at 4- μm thickness, and stained with hematoxylin and eosin (HE).

TUNEL assay

Cells were placed on cover slips in 24-well plates and infected with WSN or C-PA at an MOI of 0.01. Eight, 9, 10, 11, 12, 13, 14, 15, 16, and 24 hr after infection, cells were fixed with 1% formalin/PBS. The TUNEL assay was performed using the DeadEndTM Fluorometric TUNEL system according to the company's instructions. The samples were observed using a fluorescence microscope (Leica DM IRB, Leica, Wetzlar, Germany), and the numbers of TUNEL positive cells in 3 random fields were counted.

Caspase activity

MDCK cells were plated in 10-cm-diameter plates and infected with WSN or C-PA at an MOI of 0.01. 10 hr after infection, the cells were harvested and the activities of caspases 3, 8, and 9 measured using the Caspase-3/CPP32 Fluorometric Assay kit, the Caspase 8/FLICE Fluorometric Assay kit, and the Caspase 9 Fluorometric Assay kit (Biovision, Inc., Milpitas, USA) according to the manufacturer's instructions.

Interferon induction

Interferon induction was analyzed by measuring the luciferase activity of cells transfected with p-125Luc, which was kindly provided by Dr. Fujita [80]. 293 T cells were transfected with p-125Luc (1 μg) and pRL_{SV40} (100 ng). Four hours post-transfection, the cells were infected with WSN or C-PA at an MOI of 0.01. The interferon promoter activity was measured as the luciferase activity using the Dual-Glo luciferase assay kit and a GloMax 96 Microplate Luminometer (Promega) and normalized as the firefly luciferase/Renilla luciferase activity ratio.

Chemicals and radioisotopes

Non-radiolabeled nucleotides were purchased from GE Healthcare, [α - ^{32}P]UTP from New England Nuclear (PerkinElmer Life Sciences, Waltham, USA), and T7 RNA polymerase, T4 nucleotide kinase, oligonucleotides, human placental RNase inhibitor, and restriction enzymes from Takara (Dalian, China). The RPAIII Ribonuclease Protection Assay Kit was purchased from Ambion (Austin, USA). Anti-actin antibodies were purchased from Sigma Aldrich (St. Louis, USA). The Dual-Glo luciferase assay kit, DeadEndTM Fluorometric TUNEL system, alkaline phosphatase-conjugated anti-rabbit and anti-mouse IgG's, NBT, and BCIP were purchased from Promega. DMEM, FBS, Lipofectamine 2000, and Trizol reagent were purchased from Invitrogen.

Statistical analysis

The statistical significance levels of the data were evaluated by Student's *t*-test, with $p < 0.05$ indicating statistical significance.

Additional file

Additional file 1: Results, Methods. Figure S1. Expression of RdRp subunits and NP in the transfected cells. **Figure S2.** Time course of NP protein expression by C-PA and WSN. **Figure S3.** Time courses of NP vRNA, cRNA, and mRNA expression by C-PA and WSN.

Competing interests

The authors declare that they have no competing interests.

Author's contributions

QW, SZ, HJ, JW, LW, YM, and KX carried out the experiments. SS, FY, and MK analyzed caspase activity and mouse lung tissues. PB and VD isolated and cloned HPAIV H5N1 Cambodia. QW, SZ, SB, and TT conceived of the study. QW and SZ analyzed the data and drafted the manuscript, and SB and TT reviewed the manuscript. All authors read and approved the final manuscript.

Acknowledgements

We thank Drs. T. Fujita, G. Hobom, and Y. Kawaoka for p-125Luc, pHH21, and the influenza virus 12-plasmid reconstitution system, respectively. This work was supported by Grants-in-aid from the Chinese Academy of Sciences (0514P51131), the National Science Foundation of China (30970153), the Li Ka Shing Foundation (0682P11131), RESPARI (0581P14131), and European Union (FLUINNATE 0681P21131).

Author details

¹Units of Molecular Virology, the Key Laboratory of Molecular Virology & Immunology, Institut Pasteur of Shanghai, Chinese Academy of Sciences, 411 Hefei Road, 200025, Shanghai, P. R. China. ²Units of Viral Genome Regulation, the Key Laboratory of Molecular Virology & Immunology, Institut Pasteur of Shanghai, Chinese Academy of Sciences, 411 Hefei Road, 200025, Shanghai, P. R. China. ³Shanghai Medical College of Fudan University, Yixueyuan Road 138, Shanghai 200032, P. R. China. ⁴Roche R&D Center China LTD, 720 Cai Lun Road, Building 5, Pudong, Shanghai 201203, P. R. China. ⁵Department of Microbiology and Cell Biology, Tokyo Metropolitan Institute of Medical Biology, 3-18-22 Honkomagome, Bunkyo-Ku, Tokyo 113-8613, Japan. ⁶Institut Pasteur in Cambodia, 5 Monivong Blvd, P.O. Box 983, Phnom Penh, Cambodia. ⁷Chouju Medical Institute, Fukushima Hospital, 19-14 Azanakyama, Noyori-cho, Toyohashi, Aichi 441-8124, Japan.

Received: 14 October 2011 Accepted: 21 May 2012

Published: 8 June 2012

References

1. Webster RG, Sharp GB, Claas EC: Interspecies transmission of influenza viruses. *Am J Respir Crit Care Med* 1995, **152**:S25-30.
2. Kawaoka Y, Krauss S, Webster RG: Avian-to-human transmission of the PB1 gene of influenza A viruses in the 1957 and 1968 pandemics. *J Virol* 1989, **63**:4603-4608.
3. Lindstrom SE, Cox NJ, Klimov A: Genetic analysis of human H2N2 and early H3N2 influenza viruses, 1957-1972: evidence for genetic divergence and multiple reassortment events. *Virology* 2004, **328**:101-119.
4. Dawood FS, Jain S, Finelli L, Shaw MW, Lindstrom S, Garten RJ, Gubareva LV, Xu X, Bridges CB, Uyeki TM: Emergence of a novel swine-origin influenza A (H1N1) virus in humans. *N Engl J Med* 2009, **360**:2605-2615.
5. Wasilenko JL, Lee CW, Sarmento L, Spackman E, Kapczynski DR, Suarez DL, Pantin-Jackwood MJ: NP, PB1, and PB2 viral genes contribute to altered replication of H5N1 avian influenza viruses in chickens. *J Virol* 2008, **82**:4544-4553.
6. Huise-Post DJ, Franks J, Boyd K, Salomon R, Hoffmann E, Yen HL, Webby RJ, Walker D, Nguyen TD, Webster RG: Molecular changes in the polymerase genes (PA and PB1) associated with high pathogenicity of H5N1 influenza virus in mallard ducks. *J Virol* 2007, **81**:8515-8524.
7. Seyer R, Hrinicus ER, Ritzel D, Abt M, Mellmann A, Marjuki H, Kuhn J, Wolff T, Ludwig S, Ehrhardt C: Synergistic adaptive mutations in the hemagglutinin and polymerase acidic protein lead to increased virulence of pandemic 2009 H1N1 influenza A virus in mice. *J Infect Dis* 2012, **205**:262-271.
8. Salomon R, Franks J, Govorkova EA, Ilyushina NA, Yen HL, Huise-Post DJ, Humberd J, Trichet M, Rehg JE, Webby RJ, et al: The polymerase complex genes contribute to the high virulence of the human H5N1 influenza virus isolate A/Vietnam/1203/04. *J Exp Med* 2006, **203**:689-697.
9. Paese P, Shaw ML: Orthomyxoviridae: The Viruses and Their Replication. In *Fields Virology*, 5th edition. Edited by Knipe DM, Howley PM. Philadelphia: Lippincott Williams & Wilkins; 2007:1647-1689.
10. Toyoda T, Adyshev DM, Kobayashi M, iwata A, Ishihama A: Molecular assembly of the influenza virus RNA polymerase: determination of the subunit-subunit contact sites. *J Gen Virol* 1996, **77**(Pt 9):2149-2157.
11. Kobayashi M, Toyoda T, Ishihama A: Influenza virus PB1 protein is the minimal and essential subunit of RNA polymerase. *Arch Virol* 1996, **141**:525-539.
12. Biswas SK, Nayak DP: Mutational analysis of the conserved motifs of influenza A virus polymerase basic protein 1. *J Virol* 1994, **68**:1819-1826.
13. Ulmanen I, Broni BA, Krug RM: Role of two of the influenza virus core P proteins in recognizing cap 1 structures (m7G pppNm) on RNAs and in initiating viral RNA transcription. *Proc Natl Acad Sci U S A* 1981, **78**:7355-7359.
14. Li ML, Rao P, Krug RM: The active sites of the influenza cap-dependent endonuclease are on different polymerase subunits. *EMBO J* 2001, **20**:2078-2086.
15. Biais D, Patzelt E, Kuechler E: Cap-recognizing protein of influenza virus. *Virology* 1982, **116**:339-348.
16. Crepin T, Dias A, Palencia A, Swale C, Cusack S, Ruigrok RW: Mutational and metal binding analysis of the endonuclease domain of the influenza virus polymerase PA subunit. *J Virol* 2010, **84**:9096-9104.
17. Dias A, Bouvier D, Crepin T, McCarthy AA, Hart DJ, Baudin F, Cusack S, Ruigrok RW: The cap-snatching endonuclease of influenza virus polymerase resides in the PA subunit. *Nature* 2009, **458**:914-918.
18. Fodor E, Brownlee G: Influenza virus replication. In *Influenza*. Edited by Potter C. Amsterdam: Elsevier; 2002:1-29.
19. Hara K, Schmidt FJ, Crow M, Brownlee GG: Amino acid residues in the N-terminal region of the PA subunit of influenza A virus RNA polymerase play a critical role in protein stability, endonuclease activity, cap binding, and virion RNA promoter binding. *J Virol* 2006, **80**:7789-7798.
20. Yuan P, Barilam M, Lou Z, Chen S, Zhou J, He X, Lv Z, Ge R, Li X, Deng T, et al: Crystal structure of an avian influenza polymerase PA(N) reveals an endonuclease active site. *Nature* 2009, **458**:909-913.
21. Kawakami K, Mizumoto K, Ishihama A: RNA polymerase of influenza virus. IV. Catalytic properties of the capped RNA endonuclease associated with the RNA polymerase. *Nucleic Acids Res* 1983, **11**:3637-3649.
22. Plotch SJ, Bouloy M, Ulmanen I, Krug RM: A unique cap(m7G pppXm)-dependent influenza virion endonuclease cleaves capped RNAs to generate the primers that initiate viral RNA transcription. *Cell* 1981, **23**:847-858.
23. Krug RM, Alonso-Caplan FV, Julkunen I, Katze MG: Expression and replication of the influenza virus genome. In Edited by Krug RM. New York: Plenum Press; 1989:89-152.
24. Deng T, Vreede FT, Brownlee GG: Different de novo initiation strategies are used by influenza virus RNA polymerase on its cRNA and viral RNA promoters during viral RNA replication. *J Virol* 2006, **80**:2337-2348.
25. Zhang S, Wang J, Wang Q, Toyoda T: Internal initiation of influenza virus replication of v- and cRNA in vitro. *J Biol Chem* 2010, **285**:41194-41201.
26. Neumann G, Shinya K, Kawaoka Y: Molecular pathogenesis of H5N1 influenza virus infections. *Antivir Ther* 2007, **12**:617-626.
27. Abdel-Ghaffar AN, Chotpitayasunondh T, Gao Z, Hayden FG, Nguyen DH, de Jong MD, Naghdaliyev A, Peiris JS, Shindo N, Soeroro S, Uyeki TM: Update on avian influenza A (H5N1) virus infection in humans. *N Engl J Med* 2008, **358**:261-273.
28. Uyeki TM: Global epidemiology of human infections with highly pathogenic avian influenza A (H5N1) viruses. *Respirology* 2008, **13**(Suppl 1):S2-9.
29. Maines TR, Chen LM, Matsuoka Y, Chen H, Rowe T, Ortin J, Falcon A, Nguyen TH, le Mai Q, Sedyansingh ER, et al: Lack of transmission of H5N1 avian-human reassortant influenza viruses in a ferret model. *Proc Natl Acad Sci U S A* 2006, **103**:12121-12126.
30. Li C, Hatta M, Watanabe S, Neumann G, Kawaoka Y: Compatibility among polymerase subunit proteins is a restricting factor in reassortment between equine H7N7 and human H3N2 influenza viruses. *J Virol* 2008, **82**:11880-11888.

31. Chen LM, Davis CT, Zhou H, Cox NJ, Donis RO: Genetic compatibility and virulence of reassortants derived from contemporary avian H5N1 and human H3N2 influenza A viruses. *PLoS Pathog* 2008, **4**:e1000072.
32. Hatta M, Halfmann P, Wells K, Kawaoka Y: Human influenza A viral genes responsible for the restriction of its replication in duck intestine. *Virology* 2002, **295**:250–255.
33. Gutiérrez R, Naughtin M, Horm S, San S, Buchy P: A(H5N1) Virus Evolution in South East Asia. *Viruses* 2009, **1**:335–361.
34. Kashiwagi T, Leung BW, Deng T, Chen H, Brownlee GG: The N-terminal region of the PA subunit of the RNA polymerase of influenza A/HongKong/156/97 (H5N1) influences promoter binding. *PLoS One* 2009, **4**:e5473.
35. Fodor E, Crow M, Mingay LJ, Deng T, Sharps J, Fechter P, Brownlee GG: A single amino acid mutation in the PA subunit of the influenza virus RNA polymerase inhibits endonucleolytic cleavage of capped RNAs. *J Virol* 2002, **76**:8989–9001.
36. Hara K, Shiota M, Kido H, Ohtsu Y, Kashiwagi T, Iwashita J, Hamada N, Mizoue K, Tsumura N, Kato H, Toyoda T: Influenza virus RNA polymerase PA subunit is a novel serine protease with Ser624 at the active site. *Genes Cells* 2001, **6**:87–97.
37. Sanz-Ezquerro JJ, Zurcher T, de la Luna S, Ortin J, Nieto A: The amino-terminal one-third of the influenza virus PA protein is responsible for the induction of proteolysis. *J Virol* 1996, **70**:1905–1911.
38. Song MS, Pascua PN, Lee JH, Baek YH, Lee OJ, Kim CJ, Kim H, Webby RJ, Webster RG, Choi YK: The polymerase acidic protein gene of influenza A virus contributes to pathogenicity in a mouse model. *J Virol* 2009, **83**:12325–12335.
39. Kashiwagi T, Hara K, Nakazono Y, Hamada N, Watanabe H: Artificial hybrids of influenza A virus RNA polymerase reveal PA subunit modulates its thermal sensitivity. *PLoS One* 2010, **5**:e15140.
40. Buchy P, Mardy S, Vong S, Toyoda T, Aubin JT, Miller M, Touch S, Sovann L, Dufourcq JB, Richner B, et al: Influenza A/H5N1 virus infection in humans in Cambodia. *J Clin Virol* 2007, **39**:164–168.
41. Toyoda T, Hara K, Imamura Y: Ser624 of the PA subunit of influenza A virus is not essential for viral growth in cells and mice, but required for the maximal viral growth. *Arch Virol* 2003, **148**:1687–1696.
42. Jiang H, Zhang S, Wang Q, Wang J, Geng L, Toyoda T: Influenza virus genome C4 promoter/origin attenuates its transcription and replication activity by the low polymerase recognition activity. *Virology* 2010, **408**:190–196.
43. Reed LJ, Muench H: Simple method of estimating 50 per cent endpoints. *Amer J Hyg* 1938, **27**:493–497.
44. Wang C, Youle RJ: The role of mitochondria in apoptosis*. *Annu Rev Genet* 2009, **43**:95–118.
45. Li J, Yuan J: Caspases in apoptosis and beyond. *Oncogene* 2008, **27**:6194–6206.
46. Roulston A, Marcellus RC, Branton PE: Viruses and apoptosis. *Annu Rev Microbiol* 1999, **53**:577–628.
47. Desagher S, Martinou JC: Mitochondria as the central control point of apoptosis. *Trends Cell Biol* 2000, **10**:369–377.
48. Kroemer G: The proto-oncogene Bcl-2 and its role in regulating apoptosis. *Nat Med* 1997, **3**:614–620.
49. Kroemer G: Mitochondrial implication in apoptosis. Towards an endosymbiont hypothesis of apoptosis evolution. *Cell Death Differ* 1997, **4**:443–456.
50. Gabriel G, Dauber B, Wolff T, Planz O, Klenk HD, Stech J: The viral polymerase mediates adaptation of an avian influenza virus to a mammalian host. *Proc Natl Acad Sci U S A* 2005, **102**:18590–18595.
51. Li Z, Chen H, Jiao P, Deng G, Tian G, Li Y, Hoffmann E, Webster RG, Matsuoka Y, Yu K: Molecular basis of replication of duck H5N1 influenza viruses in a mammalian mouse model. *J Virol* 2005, **79**:12058–12064.
52. Hatta M, Gao P, Halfmann P, Kawaoka Y: Molecular basis for high virulence of Hong Kong H5N1 influenza A viruses. *Science* 2001, **293**:1840–1842.
53. Gabriel G, Herwig A, Klenk HD: Interaction of polymerase subunit PB2 and NP with importin alpha1 is a determinant of host range of influenza A virus. *PLoS Pathog* 2008, **4**:e11.
54. Mehle A, Doudna JA: An inhibitory activity in human cells restricts the function of an avian-like influenza virus polymerase. *Cell Host Microbe* 2008, **4**:111–122.
55. Mehle A, Doudna JA: Adaptive strategies of the influenza virus polymerase for replication in humans. *Proc Natl Acad Sci U S A* 2009, **106**:21312–21316.
56. Neumann G, Watanabe T, Ito H, Watanabe S, Goto H, Gao P, Hughes M, Perez DR, Donis R, Hoffmann E, et al: Generation of influenza A viruses entirely from cloned cDNAs. *Proc Natl Acad Sci U S A* 1999, **96**:9345–9350.
57. Sarmiento L, Afonso CL, Estevez C, Wasilenko J, Pantin-Jackwood M: Differential host gene expression in cells infected with highly pathogenic H5N1 avian influenza viruses. *Vet Immunol Immunopathol* 2008, **125**:291–302.
58. Vester D, Rapp E, Gade D, Genzel Y, Reichl U: Quantitative analysis of cellular proteome alterations in human influenza A virus-infected mammalian cell lines. *Proteomics* 2009, **9**:3316–3327.
59. Kato H, Takeuchi O, Sato S, Yoneyama M, Yamamoto M, Matsui K, Uematsu S, Jung A, Kawai T, Ishii KJ, et al: Differential roles of MDAS and RIG-I helicases in the recognition of RNA viruses. *Nature* 2006, **441**:101–105.
60. Loo YM, Fornek J, Crochet N, Bajwa G, Perwitasari O, Martinez-Sobrido L, Akira S, Gill MA, Garcia-Sastre A, Katze MG, Gale M Jr: Distinct RIG-I and MDAS signaling by RNA viruses in innate immunity. *J Virol* 2008, **82**:335–345.
61. Yoneyama M, Fujita T: RNA recognition and signal transduction by RIG-I-like receptors. *Immunol Rev* 2009, **227**:54–65.
62. Rehwinkel J, Tan CP, Goubau D, Schulz O, Pichlmair A, Bier K, Robb N, Vreede F, Barclay W, Fodor E, Reis E, Sousax C: RIG-I detects viral genomic RNA during negative-strand RNA virus infection. *Cell* 2010, **140**:397–408.
63. Haller O, Kochs G, Weber F: The interferon response circuit: induction and suppression by pathogenic viruses. *Virology* 2006, **344**:119–130.
64. Taniguchi T, Takaoka A: The interferon-alpha/beta system in antiviral responses: a multimodal machinery of gene regulation by the IRF family of transcription factors. *Curr Opin Immunol* 2002, **14**:111–116.
65. Price GE, Gaszewska-Mastariar A, Moskophidis D: The role of alpha/beta and gamma interferons in development of immunity to influenza A virus in mice. *J Virol* 2000, **74**:3996–4003.
66. Mosca JD, Pitha PM: Transcriptional and posttranscriptional regulation of exogenous human beta interferon gene in simian cells defective in interferon synthesis. *Mol Cell Biol* 1986, **6**:2279–2283.
67. Kuchipudi SV, Dunham SP, Nelij R, White GA, Coward VJ, Siomka MJ, Brown IH, Chang KC: Rapid death of duck cells infected with influenza: a potential mechanism for host resistance to H5N1. *Immunol Cell Biol* 2011.
68. Brydon EW, Morris SJ, Sweet C: Role of apoptosis and cytokines in influenza virus morbidity. *FEMS Microbiol Rev* 2005, **29**:837–850.
69. Olsen CW, Kehren JC, Dybdahl-Sissoko NR, Hinshaw VS: bcl-2 alters influenza virus yield, spread, and hemagglutinin glycosylation. *J Virol* 1996, **70**:663–666.
70. Wurzer WJ, Planz O, Ehrhardt C, Giner M, Silberzahn T, Pleschka S, Ludwig S: Caspase 3 activation is essential for efficient influenza virus propagation. *EMBO J* 2003, **22**:2717–2728.
71. McLean JE, Datan E, Matassov D, Zakeri ZF: Lack of Bax prevents influenza A virus-induced apoptosis and causes diminished viral replication. *J Virol* 2009, **83**:8233–8246.
72. Machida K, Tsukiyama-Kohara K, Seike E, Tone S, Shibasaki F, Shimizu M, Takahashi H, Hayashi Y, Funata N, Taya C, et al: Inhibition of cytochrome c release in Fas-mediated signaling pathway in transgenic mice induced to express hepatitis C viral proteins. *J Biol Chem* 2001, **276**:12140–12146.
73. Pe'ery T, Mathews M: Viral translational strategies and host defense mechanism. In *Translational Control of Gene Expression*. Edited by Sonenberg N, Hershey J, Mathews M. Cold Spring Harbor: Cold Spring Harbor Laboratory Press; 2000:371–424.
74. McLean JE, Ruck A, Shirazian A, Pooyaei-Mehr F, Zakeri ZF: Viral manipulation of cell death. *Curr Pharm Des* 2008, **14**:198–220.
75. Zamarin D, Garcia-Sastre A, Xiao X, Wang R, Palese P: Influenza virus PB1-F2 protein induces cell death through mitochondrial ANT3 and VDAC1. *PLoS Pathog* 2005, **1**:e4.
76. Zamarin D, Ortigoza MB, Palese P: Influenza A virus PB1-F2 protein contributes to viral pathogenesis in mice. *J Virol* 2006, **80**:7976–7983.
77. Zhang S, Wang Q, Wang J, Mizumoto K, Toyoda T: Two mutations in the C-terminal domain of influenza virus RNA polymerase PB2 enhance transcription by enhancing cap-1 RNA binding activity. *Biochim Biophys Acta* 2012, **1819**:78–83.
78. Zhang S, Weng L, Geng L, Wang J, Zhou J, Deubei V, Buchy P, Toyoda T: Biochemical and kinetic analysis of the influenza virus RNA polymerase purified from insect cells. *Biochem Biophys Res Commun* 2010, **391**:570–574.

79. Goto H, Wells K, Takada A, Kawaoka Y: Plasminogen-binding activity of neuraminidase determines the pathogenicity of influenza A virus. *J Virol* 2001, **75**:9297–9301.
80. Yoneyama M, Suhara W, Fukuhara Y, Sato M, Ozato K, Fujita T: Autocrine amplification of type I interferon gene expression mediated by interferon stimulated gene factor 3 (ISGF3). *J Biochem* 1996, **120**:160–169.

doi:10.1186/1743-422X-9-106

Cite this article as: Wang *et al.*: PA from an H5N1 highly pathogenic avian influenza virus activates viral transcription and replication and induces apoptosis and interferon expression at an early stage of infection. *Virology Journal* 2012 **9**:106.

**Submit your next manuscript to BioMed Central
and take full advantage of:**

- Convenient online submission
- Thorough peer review
- No space constraints or color figure charges
- Immediate publication on acceptance
- Inclusion in PubMed, CAS, Scopus and Google Scholar
- Research which is freely available for redistribution

Submit your manuscript at
www.biomedcentral.com/submit



Self-Enhancement of Hepatitis C Virus Replication by Promotion of Specific Sphingolipid Biosynthesis

Yuichi Hirata¹, Kazutaka Ikeda^{2,3}, Masayuki Sudoh⁴, Yuko Tokunaga¹, Akemi Suzuki⁵, Leiyun Weng⁶, Masatoshi Ohta³, Yoshimi Tobita¹, Ken Okano⁷, Kazuhisa Ozeki⁷, Kenichi Kawasaki⁴, Takuo Tsukuda⁴, Asao Katsume⁴, Yuko Aoki⁴, Takuya Umehara¹, Satoshi Sekiguchi¹, Tetsuya Toyoda⁶, Kunitada Shimotohno⁸, Tomoyoshi Soga³, Masahiro Nishijima^{9,10}, Ryo Taguchi^{2,11}, Michinori Kohara^{1*}

1 Department of Microbiology and Cell Biology, Tokyo Metropolitan Institute of Medical Science, Setagaya-ku, Tokyo, Japan, **2** Department of Metabolome, Graduate School of Medicine, The University of Tokyo, Bunkyo-ku, Tokyo, Japan, **3** Institute for Advanced Biosciences, Keio University, Kakuganji, Tsuruoka, Yamagata, Japan, **4** Kamakura Research Laboratories, Chugai Pharmaceutical Co., Ltd., Kamakura, Kanagawa, Japan, **5** Institute of Glycoscience, Tokai University, Hiratsuka-shi, Kanagawa, Japan, **6** Unit of Viral Genome Regulation, Institut Pasteur of Shanghai, Key Laboratory of Molecular Virology & Immunology, Chinese Academy of Sciences, Shanghai, China, **7** Fuji-Gotemba Research Laboratories, Chugai Pharmaceutical Co., Ltd., Gotemba, Shizuoka, Japan, **8** Research Institute, Chiba Institute of Technology, Narashino, Chiba, Japan, **9** National Institute of Health Sciences, Setagaya-ku, Tokyo, Japan, **10** Showa Pharmaceutical University, Machidashi, Tokyo, Japan, **11** Department of Biomedical Sciences, College of Life and Health Sciences, Chubu University, Kasugai-shi, Aichi, Japan

Abstract

Lipids are key components in the viral life cycle that affect host-pathogen interactions. In this study, we investigated the effect of HCV infection on sphingolipid metabolism, especially on endogenous SM levels, and the relationship between HCV replication and endogenous SM molecular species. We demonstrated that HCV induces the expression of the genes (*SGMS1* and *2*) encoding human SM synthases 1 and 2. We observed associated increases of both total and individual sphingolipid molecular species, as assessed in human hepatocytes and in the detergent-resistant membrane (DRM) fraction in which HCV replicates. *SGMS1* expression had a correlation with HCV replication. Inhibition of sphingolipid biosynthesis with a hepatotropic serine palmitoyltransferase (SPT) inhibitor, NA808, suppressed HCV-RNA production while also interfering with sphingolipid metabolism. Further, we identified the SM molecular species that comprise the DRM fraction and demonstrated that these endogenous SM species interacted with HCV nonstructural 5B polymerase to enhance viral replication. Our results reveal that HCV alters sphingolipid metabolism to promote viral replication, providing new insights into the formation of the HCV replication complex and the involvement of host lipids in the HCV life cycle.

Citation: Hirata Y, Ikeda K, Sudoh M, Tokunaga Y, Suzuki A, et al. (2012) Self-Enhancement of Hepatitis C Virus Replication by Promotion of Specific Sphingolipid Biosynthesis. *PLoS Pathog* 8(8): e1002860. doi:10.1371/journal.ppat.1002860

Editor: Aleem Siddiqui, University of California, San Diego, United States of America

Received: January 4, 2012; **Accepted:** June 27, 2012; **Published:** August 16, 2012

Copyright: © 2012 Hirata et al. This is an open-access article distributed under the terms of the Creative Commons Attribution License, which permits unrestricted use, distribution, and reproduction in any medium, provided the original author and source are credited.

Funding: This study was supported by grants from the Ministry of Education, Culture, Sports, Science, and Technology of Japan; the Program for Promotion of Fundamental Studies in Health Science of the National Institute of Biomedical Innovation of Japan; and the Ministry of Health, Labor, and Welfare of Japan. The funders had no role in study design, data collection and analysis, decision to publish, or preparation of the manuscript.

Competing Interests: M. Sudoh, A. Katsume, K. Okano, K. Ozeki, K. Kawasaki, T. Tsukuda, and Y. Aoki are employees of Chugai Pharmaceutical Co. Ltd. This does not alter our adherence to all PLoS Pathogens policies on sharing data and materials.

* E-mail: kohara-mc@igakuken.or.jp

Introduction

Lipids have long been known to play dual roles in biological systems, functioning in structural (in biological membranes) and energy storage (in cellular lipid droplets and plasma lipoproteins) capacities. Research over the past few decades has identified additional functions of lipids related to cellular signaling, microdomain organization, and membrane traffic. There are also strong indications of the important role of lipids in various stages of host-pathogen interactions [1].

Sphingomyelin (SM) is a sphingolipid that interacts with cholesterol and glycosphingolipid during formation of the raft domain, which can be extracted for study as a detergent-resistant membrane (DRM) fraction [2]. Recently, raft domains have drawn attention as potential platforms for signal transduction and pathogen infection processes [3,4]. For instance, raft domains may serve as sites for hepatitis C virus (HCV) replication [5,6]. Additionally, *in vitro* analysis indicates that synthetic SM binds to

the nonstructural 5B polymerase (RdRp) of HCV [7]. This association allows RdRp to localize to the DRM fraction (known to be the site of HCV replication) and activates RdRp, although the degree of binding and activation differs among HCV genotypes [7,8]. Indeed, suppression of SM biosynthesis with a serine palmitoyltransferase (SPT) inhibitor disrupts the association between RdRp and SM in the DRM fraction, resulting in the suppression of HCV replication [7,9].

Multiple reports have indicated that HCV modulates lipid metabolism (e.g., cholesterol and fatty acid biosynthesis) to promote viral replication [10–12]. However, the effect of HCV infection on sphingolipid metabolism, especially on endogenous SM levels, and the relationship between HCV replication and endogenous SM molecular species remain to be elucidated as there are technical challenges in measuring SM levels (for both total and individual molecular species) in hepatocytes.

To address these questions, we first utilized mass spectrometry (MS)-based techniques and analyzed uninfected and HCV-